ALFRED-WEGENER-INSTITUT
HELMHOLTZ-ZENTRUM FÜR POLAR- UND MEERESFORSCHUNG

Hochschule Bremerhaven

BACHELOR'S THESIS

Developing artificial collectors for growth monitoring of biofouling communities in the southern German Bight – North Sea

University of Applied Sciences Bremerhaven

Biotechnology of Marine Resources (BMR)

Rike Düffert

36328

20.12.2022

First Supervisor: Prof. Dr. Bela H. Buck

Second Supervisor: Dr. Wolf Isbert

Affidavit

I, Rike Düffert, hereby declare that I have written this thesis independently and have not used any aids or sources other than those indicated. I have marked any material that I have taken over verbatim or in substance.

Driftsethe, 20.12.2022 R. Düffert

Place, date of submission Signature

Zusammenfassung

Im Hinblick auf die Klimakrise, entwickelt sich vor allem die Offshore-Windenergie zu einer immer bedeutsameren nachhaltigen Ressource zur Energiegewinnung um fossile Brennstoffe in der Zukunft abzulösen. Dabei erzielen die Fundamente der einzelnen Windkraftanlagen einen Riff-Effekt und werden zur Ansiedlungsstelle für Organismen, welche auf dem überwiegend sandigen Meeresboden der südlichen Nordsee natürlicherweise nicht vorkommen würden. Durch diese künstlichen Hartsubstrate können Ansiedlungs- und Entwicklungsprozesse von sogenannten Biofouling Organsimen beobachtet und dokumentiert werden. Während des Baus solcher Anlagen müssen durch Aufwuchsorganismen entstehende Last-Beiwerte berücksichtigt werden, die bisher immer abgeschätzt wurden, da keine geeigneten Studien zur genauen Berechnung der Werte existieren. Daher wird im Rahmen des *EnviSim4Mare* Projekts erstmalig in Deutschland ein Meerwasserwellen- und Strömungskanal konstruiert um Messungen an geeigneten Testkörpern mit Bewuchs durchzuführen. Um eine standardisierte Probennahme zur Evaluation von Foulinggemeinschaften gewährleisten zu können, wurden zwei künstliche Hartsubstrate entwickelt, die an einem exponierten (Nordergründe Windpark) und geschützten Standort (Nord-Ost Hafen von Helgoland) deponiert wurden.

In dieser Bachelorarbeit werden die zusammengetragenen Ergebnisse der Entwicklung (mit Rücksicht auf unterschiedliche Umweltbedingungen) Ausbringung, der Handhabung während der Probennahmen sowie der sich entwickelten Aufwuchsgemeinschaften beider Systeme vorgestellt und diskutiert. Dabei wurde ein Beprobungszeitraum von zwei Jahren (Mai bis Dezember 2021 und April bis Oktober 2022) berücksichtigt. Die Überwachung unter realen Bedingungen der Biofoulinggemeinschaften soll Aufschluss über saisonale und räumliche Ansiedlungsprozesse sowie Zusammensetzung individueller Taxa geben und zeigen, welche Organismen dominierende Charakteristika aufweisen. Dabei wurde zwischen den beiden Standorten in drei Habitate unterschieden: Nordergründe Sublitoral (Unterwasser), Helgoland Eulitoral (Gezeitenzone) und Helgoland Sublitoral. Durch morpho-taxonomische Auswertungen konnten drei Biofouling Gemeinschaften identifiziert werden, die sich vor allem in ihrem Standort unterscheiden und durch spezifische abiotische Faktoren gekennzeichnet sind.

Abstract

With regard to the current climate crisis, offshore wind energy in particular is developing into an increasingly important sustainable resource for energy production in order to replace fossil fuels in the future. The foundations of the individual wind turbines create a reef effect and provide a habitat for organisms that would not naturally occur on the predominantly sandy seabed of the southern North Sea. Through artificial hard substrates, settlement and development processes of so-called biofouling organisms can be observed and documented. During the construction of such plants, load coefficients caused by fouling organisms have to be taken into account. Until now, these load coefficients have always been estimated, since no suitable studies exist to calculate the values accurately. Therefore, within the *EnviSim4Mare* project, a seawater wave and flow channel is constructed for the first time in Germany to perform measurements on suitable test bodies with fouling. To ensure standardized sampling for the evaluation of fouling communities, two artificial hard substrates were developed and deposited at an exposed offshore (Nordergründe wind farm) and sheltered site (north-east harbour of Helgoland).

This bachelor thesis presents and discusses the compiled results of the development (with consideration of different environmental conditions) deployment, handling during sampling as well as the developed emergent communities of the two systems. A sampling period of two years (May to December 2021 and April to October 2022) was considered. Monitoring under real conditions of biofouling communities will provide information on the seasonal and spatial settlement processes as well as composition of individual taxa and show which organisms exhibit dominant characteristics. Three habitats were distinguished between the two sites: Nordergründe sublittoral (underwater), Helgoland eulittoral (intertidal) and Helgoland sublittoral. Through morpho-taxonomic analyses three biofouling communities were identified, which differ mainly in their location and are characterized by specific abiotic factors.

Table of Contents

Figure Index

List of Tables

Abbreviation Index

AWI……Alfred-Wegener-Institute for Polar- and Marine Research

BMWK..... German Federal Ministry for Economic Affairs and Energy

EEZ..... Exclusive Economic Zone

GW.....Gigawatt

LWI ..... Leichtweiss Institute of Hydraulic Engineering

MRE.....Marine renewable energy

PE ..... Polyethylene

RAS .....Recirculating Aquaculture System

SST.....Surface Sea Temperature

SWWC .....Seawater wave and current flume

WSA..... Federal Waterways and Shipping Administration

ZAF .....Centre for Aquaculture Research

1 Introduction

According to Deutsche WindGuard (2022) 1.501 windmills in 18 offshore[1] wind farms were connected to the grid in June 2022 in the North- and Baltic Sea; together, they generated approximately 7.794 megawatts. By comparison, Germany's remaining nuclear power plants had an average output of 4.291 megawatts in 2022 (KernD 2022). It is expected that offshore windmills with a total capacity of 20 gigawatt (GW) will be in operation off the coasts of Germany by 2030 (Windenergie 2021). This will supply up to 20 million households with electricity which corresponds to about half of all German households (41,5 Mio in 2019; BPB 2019). Consequently, offshore wind energy is an increasingly important component in replacing key energy resources based on fossil fuels. Wind farms produce electricity at almost any time of day or night, allowing them to reach the same number of operating hours as commercial coal-fired power plants (IWR 2022). Likewise, the German government's goal is to increase the installed capacity of offshore wind power from today's 7.8 GW to 70 GW by 2045, making an even greater contribution to the energy transition (IWR 2022).

The southern North Sea is mainly characterized by muddy and sandy bottoms (soft bottoms), with few areas of hard substrata only, e.g. the island of Helgoland (Beermann & Franke 2011). The newly created artificial hard substrata provided by e.g. windmill foundations and the surrounding scour protection[2] to avoid erosion of sediments quickly become a new settlement area for various species of benthic organisms, commonly referred to as biofouling (Lincoln et al 1998). Biofouling poses a major challenge in terms of service life and functionality of those windmills. As it adds in weight, thickness and surface roughness increases, which modifies the hydrodynamic load on the materials and can promote corrosion (Jusoh & Wolfram 1996; Loxton et al 2017). Antifouling treatments, such as special coatings for ships, are not suitable for most large artificial structures as they have to be repainted over time, which is often logistically unfeasible (Hopkins et al 2021). These offshore structures have to be inspected and possibly cleaned repeatedly in order to guarantee their function, resulting in higher maintenance costs (Klijnstra et al 2017). Likewise, safe ascent and descent for employees must be guaranteed when working at the windmills (Klijnstra et al 2017). A preventive measure in the construction of windmills and its foundations is based on heightened design criteria

[1] Between more than 12 nautical miles (22.2 km; Böttcher 2013) and a minimum of three nautical miles (5.6 km; Jahn 2020).

[2] Erosion protection, deepening around the foundation caused by flow/currents

building those more robust to withstand fouling in terms of load-bearing capacity and safety (Klijnstra et al 2017).

The expected ecological effects of offshore wind farms on benthic communities are diverse, while e.g. windmill foundations will act as artificial reef (*reef effect,* Dannheim 2015). New reefs bring more faunal diversity in present soft bottom communities, becoming a transitional diversity hotspot in rather sparse surroundings (Langhamer et al 2009; Krone et al 2013). Resulting reefs can become a new habitat for benthic organisms as well as feeding grounds and shelter for species e.g. fish or seals (Krone et al 2013). Windmill foundations are mostly recruited by opportunistic, e.g. r-strategists, which reproduce in short-living cycles for rapid settlement. In the immediate vicinity of the windmills, change in hydrography, sediment composition and geochemistry may occur and consequently, the detrimental restructuring of soft bottom communities (Dannheim 2015). Additionally, local soft-bottom species might no longer be able to settle in the immediate vicinity of the piles due to a more heterogenous stratification of the sediment (Orejas et al 2005).

Biofouling research is fundamental for growing sectors like marine renewable energy (MRE), where devices are partly composed of moving components and/or new materials which have never been deployed in marine environments (Want et al 2017; Want & Porter 2018). With its damaging properties, developing biofouling communities represent a relevant and dynamic process for the functioning, resistance and longevity of any artificial structure at sea, starting the fouling development process with the very first water contact (Vinagre et al 2020).

For the estimation of hydrodynamic forces (waves, currents) and its impacts on cylindric (windmill) foundations the Morison equation **Equation (1)** is commonly used, comprising the specified coefficients for drag and inertia also assessing the effects of surface roughness (biofouling) (Al-Yacouby et al 2014; Morison et al 1950). Marine growth is taken into account with dimensionless coefficients for wave and current loads. But in practice, the coefficients are often selected with a high degree of certainty due to a lack of detailed knowledge (Goseberg 2019).

The *EnviSim4Mare*[3] (Experimental Investigations of Marine Growth on Test Bodies) research project is a joint project of the Leichtweiss Institute of Hydraulic Engineering (LWI) at the Technical University of Braunschweig, the Alfred-Wegener-Institute Helmholtz-Centre for Polar- and Marine Research (AWI) and the two companies Jörss-

[3] Funded by the German Federal Ministry for Economic Affairs and Climate Action (BMWK; FKZ03SX495-B)

Blunck-Ordemann GmbH and Ocean Breeze Energy GmbH & Co. KG. The first aim of this research project is the investigation of force coefficients based on real living marine growth on the test bodies in the laboratory, providing more precise information on the loads and load flows. The potential impact of biofouling on artificial structures shall be assessed by measurement trials in the first seawater wave and current flume (SWWC-flume) in Germany (TU Braunschweig). For these measurement trials stainless-steel test bodies were deployed at suitable locations in the southern North Sea (German bight) to gather natural fouling organisms. The knowledge of fluctuation ranges of those force coefficients will provide improved guidelines for the dimensioning of future windmills and for service life considerations such as recalculations, whereas operating concepts will be improved and calculated in a cost-optimized manner.

The second project aim includes the monitoring of fouling community development growing on test bodies (stainless-steel panels) under different environmental conditions; exposed in the Nordergründe wind farm area and sheltered in the north-east harbour at the island of Helgoland on permanently moored systems. Artificial structures for the collection and sampling of biofouling were developed and deployed to compare the composition of those communities spatially and seasonally under real environmental and biological conditions over time. In addition, a closed Recirculating Aquaculture System (RAS) was developed and installed at the Centre for Aquaculture Research (ZAF, AWI, Bremerhaven), to maintain living organisms alive after sampling until further evaluation, including taxonomic species identification.

In this thesis the development, deployment and handling during sampling procedure of the two different sampling devices *System A* (offshore test facility at the Nordergründe wind farm site) and *System B* (nearshore[4] test facility at the Island of Helgoland, north-east yacht harbour) are described, compared and shall be discussed in their technical functionality with regards their fouling community's growth between May 2021 and October 2022.

1.1 Background

The biofouling process starts within minutes after the immersion of any artificial structure in water with the adhesion of dissolved organic particles, forming a biofilm of proteins, polysaccharides and proteoglycan (Wahl 1989). Shortly after, single-celled bacteria and diatoms, so-called primary colonizers (Abarzua & Jakubowski 1995), settle on the

[4] Zone between land and *offshore* is defined as *nearshore* (Jahn 2020)

surface, constituting a primary film (slime film) **Figure 1** (Wahl 1989). This process is followed by Protozoa (e.g. Ciliata) and macroalgae spores settlement after roughly 24 hours (Abaruza & Jakubowski 1995). Latter constitute the secondary colonizers **Figure 1** in the process of microfouling, while algae spores also represent the interstage into macrofouling (Abarzua & Jakubowski 1995; Caspers 1952). Two to three weeks later sessile macro foulants (tertiary colonizers), larvae of sessile organisms such as tunicates, bryozoans, barnacles, mussels, polychaetes, attach to the microfouling film (Abaruza & Jakubowski; Tanaka & Asakawa 1988) **Figure 1**. After months to a few years, a diverse fouling community eventually arises, characterized by a biodiversity of sessile and vagile epibenthic fouling organisms whose constitution will constantly change in succession over time (Vinagre et al 2020).

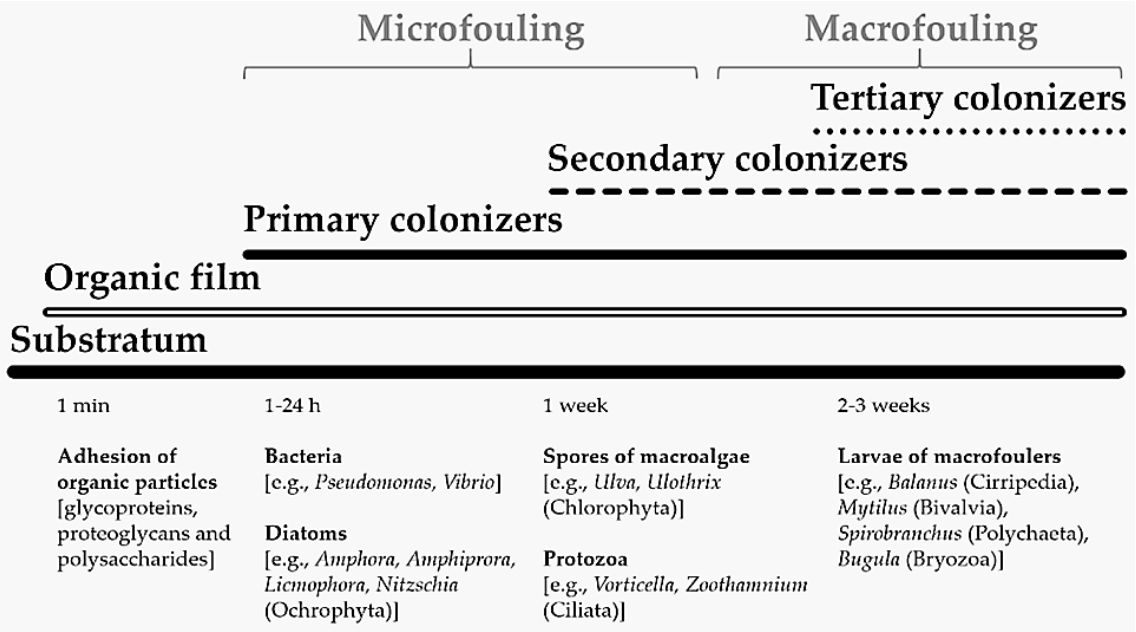

Figure 1 Succession model with the four phases of biofouling development (Wahl 1989).

As these communities grow and age, macro foulants provide secondary micro habitats, which attract further fouling (Railkin 2003). A fouling communities' succession process, formation and composition is often different and variable since it is shaped by various abiotic and biotic factors (Klijnstra et al 2017; Railkin 2013). Biofouling varies geographically, as well as locally and seasonally (Vinagre et al 2020). Abiotic environmental factors comprise temperature, salinity, pH, and nutrient content of the water. In temperate areas e.g. the North Sea with mild temperatures (5-20 °C), biofouling is strongly characterized by seasonality in spawning and growth occurring from spring

(beginning of April) to early fall (early October) (Hellio & Yebra 2009; Lehaitre et al 2008; Vinagre et al 2020). Further, nutrient contents rise with the summer season, increasing fouling biomass on artificial structures (Almeida & Coolen 2020; Momber et al 2015). Hydrodynamic characteristics comprise tides, currents, waves as well as distance from shore and seabed topography, whereas filtrating organisms like mussels, barnacles and tubeworms benefit from currents, as they feed on particulate organic matter (Railkin 2003). Many larvae of invertebrates and spores of algae are carried offshore by currents, whereas the closer the artificial structure to the shore, the higher is the probability of settlement (Almeida & Coolen 2020). The material composition (e.g. metal vs. plastic), colour, roughness, period of submersion and mobility of the construction, e.g. free moving equipment such as tidal turbines or static structures e.g. windmill foundations, influence settlement and growth of fouling communities (Cao et al 2011; Lehaitre et al 2008; Van der Stap et al 2016). Previous studies showed that aluminium, carbon, steel and bronze are more susceptible to biofouling than some non-metallic substrata such as glass fibre, polyethylene, and rubber (Pomerat et al 1946, Titah-Benbouzid et al 2017). Among biotic factors, the biology and interaction between the individual species that colonize determines whether settlement can take place at all (Vinagre et al 2020). The competition for space, food supply, reproduction opportunities and predator-prey relationship ultimately determine which species will settle (Dayton 1971; Johnson & Strathmann 1989; Raffaelli & Hawkins 1999). Further, over settlement will take place at some point, where the under most layer of the fouling community is overgrown by another layer of biofouling organisms, hence nutritional supply is no longer provided and organisms may decrease, fall off and create new settlement areas (Kerckhof et al 2019; Raffaelli & Hawkins 1999). Many of these factors are interrelated as well as under seasonal and local influences (Vinagre et al 2020). So far, over 4000 different marine organisms have been classified as biofouling organisms globally (Cao et al 2011; Yebra et al 2004). Less diverse, more abundant macro foulants make up the majority of the detected weight and/or mostly affecting hydrodynamic load and thickness. Five groups have been identified as those causing the greatest impacts on artificial offshore MRE structures: kelp (soft-fouling), bryozoans (soft- to hard-fouling, depending on species), mussels, acorn barnacles and calcareous tube-worms (all hard-fouling) (Richmond & Seed 1991).

Morison-equation

In the appraisal of loads and load flows (wave, currents) the potential impact caused by fouling communities (drag forces) on artificial structures e.g. windmill foundations, is considered by establishing dimensionless coefficients for drag and inertia within the following formula developed by Morison (1950).

$$F = \rho C_m D^2 \frac{\pi}{4} \dot{u} + \frac{1}{2} \rho C_d D |u| u \qquad \textbf{(1)}$$

In equation **(1)**: F – total fluid force (per unit length) on the pile, ρ – density of water, C_m – inertia coefficient for the body (mass), D – pile diameter, $\dot{u} = du/dt$ – flow acceleration, C_d – drag coefficient for the body, u – flow velocity.

1.2 Study sites

Both selected study sites, with different environmental conditions, Nordergründe wind farm area and the Island of Helgoland, are located within the southern North Sea, in the coastal zone of the German Bight **Figure 2**.

Figure 2 Both study sites marked with Nor=Nordergründe wind farm site and Hel=Helgoland within the coastal zone of the southern German Bight (Hannemann 2022).

The North Sea is one of the largest shelf seas in the world, with inflow from the Atlantic Ocean through the Fair Isle Channel, over the East Shetland Shelf, the Dover Straight between Great-Britain and France, as well as from the western flank of the Norwegian Channel (Huthnance 1991). The outflow runs parallel to the Norwegian coast over the Norwegian Channel (Huthnance 1991). Additionally, a fluctuating exchange of salt- and fresh water from the Baltic Sea runs through the Skagerrak between Norway and Denmark. The bathymetry of the German Bight is characterized by the extensive shallow Wadden Sea, which covers a total area of over 8,000 km² and a width of up to 40 km, off the Frisian coast (Becker et al 1992). The southern North Sea is shaped by the distinct post-glacial valley of the Elbe River as well, which extends north-westward from its estuary and passes the *Dogger Bank* on the eastern side of Tail End (Becker et al 1992). In general, water depths increase with distance from the coast; within the German Bight, the greatest water depth is 56 m in the *Tiefe Rinne*, located southwest of Helgoland. In the north-western most tip of the German Exclusive Economic Zone (EEZ), the ***duck's beak***, the water depth reaches slightly more than 60 m (BMU 2018). The hydrodynamics of the North Sea are significantly influenced by semi-diurnal astronomical tides (co-oscillations with autonomous tidal waves) of the Atlantic which enter the North Sea basin counter-clockwise, the North Sea is too small for a direct effect of tidal potential (Jänicke 2021). The characteristic geometry of the North Sea basin implies intrinsic periods causing a significant spring-nap-rhythm, which induces strong tidal currents and high velocities with turbulent vertical and horizontal exchange. This provides a well-mixed water mass and prevents a lack of stratification in the shallow southern North Sea (Becker et al 1992; Sündermann & Pohlmann 2011). In the Wadden Sea, tides cause the periodic exposure of large areas of seafloor (Becker et al 1992; Sündermann & Pohlmann 2011). The potential tidal range lies between 1-5 m (Quante & Colin 2016), with an average tidal range of 2.28 m in the German Bight (Becker et al 1992).

The North Sea area is equally characterized by intense storms, mainly occurring from September to April (Bell et al 2017), including storms with wind strengths of ≥ 8 Beaufort[5] and wave heights of ≥4 m, showing a significant maximum in November (Korevaar 1990). Early summers (May to June) are usually characterized by low wind situations (≤ 2 Beaufort) and calm sea states with wave heights of less than 1.5 m (Korevaar 1990; Weisse & Günther 2007).

[5] The Beaufort scale (Bft) divides wind force into 13 strength ranges from 0 (calm) to 12 (hurricane) (Deutscher Wetterdienst 2022).

In shallower areas of the German Bight, such as the reef bottoms off the island of Borkum, the benthos is characterized by a heterogeneous sediment distribution with predominantly medium to large sandy sediment (Figge 1981). With increasing water depth, medium to fine sandy sediments predominate, with 10-20% clay and silt content (Figge 1981). The outer reefs off the islands of Sylt and Helgoland are characterized by a pronounced heterogeneous sediment distribution with residual or relict sediments (coarse sands, gravels and stones) (Figge 1981). The sediments in the area of the Elbe glacial valley and of the *duck's beak* consist of sands with silt and clay fractions, which can rise to 50 % with increasing water depth in some areas (Figge 1981).

2 Material and Methods

2.1 Study site Nordergründe

To obtain results regarding succession patterns and development under realistic environmental conditions **Table 1**, similar to those found at offshore windmill foundations, *System A* (position: 53° 50.40902' N; 008° 11.59697' E) was located in the immediate vicinity of the offshore wind farm *Nordergründe* (18 monopiles, 110 Megawatt, area of 3.5 km^2; BMWE 2021).

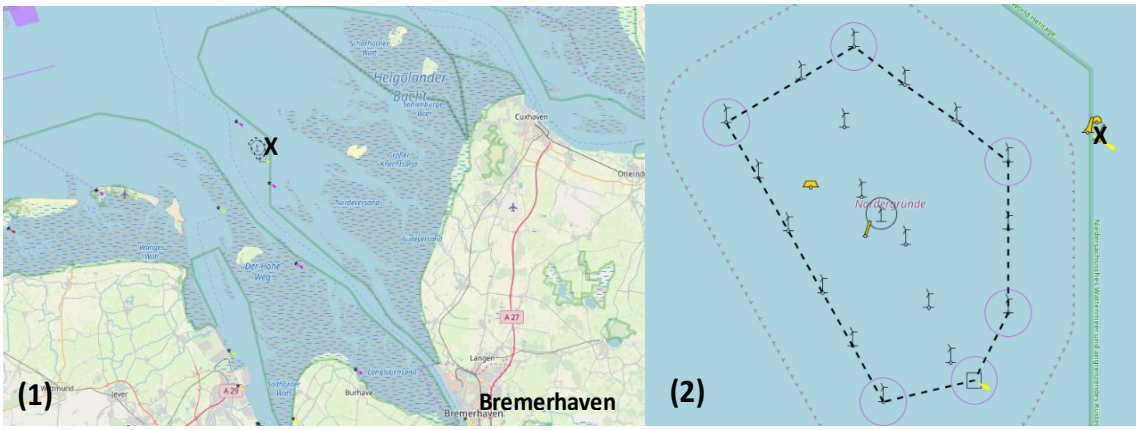

Figure 3 (1) Nordergründe wind farm indicated with (X). **(2)** System A moored in the northeast of the wind farm, indicated with (X) (Hannemann 2022).

The wind farm is located approximately 30 km off the coast of Bremerhaven (BMWE 2021) in the shallower Nordergründe area, within the south-eastern German Bight **Figure 3**. It was important that the study site is located offshore but being also logistically accessible within one day for regular samplings.

The Nordergründe area in general is characterized by shoals, sandbanks and gullies and water depths range from 3 to 22 m (BSH 2019; Dörjes et al 1970). Mean tidal range in this area is about 3 m (Jänicke et al 2021), while the measured maximum surface currents at the Nordergründe location range from 0.6 to 1.5 m/s (Dörjes et al 1970; Buck 2007). The main direction of the current ranges from northwest to southeast and reverses depending on the tidal state (Buck 2007). Wave heights were measured below 1 m (January to December 2021) but maximum wave heights over 6 m may occur during storms (Buck 2007). Nordergründe area sediment loads are dominated by fine sand with varying parts of silt and medium sand (Dörjes et al 1970; Zeiler et al 2018). The site is under the influence of the estuaries of the Jade, the Elbe and Weser River, with an observed highly dynamic sediment transport and freshwater input (Putzar & Macherek 2015). Data on temperature recorded at the *Alte Weser* lighthouse located within the Nordergründe area shows minimum and maximum values of -0.1 and 21.7 °C (mean 11.1 ± 5.6 °C, values taken from January 2010-December 2020). Salinity values were measured at the same location with a minimum of 25.7 g/kg and a maximum of 34.3 g/kg (mean 30.8 ± 1.2 g/kg; values from January 2010-December 2020), respectively (WSA, 2021).

2.2 Study site Helgoland

System B (position: 54°11'03.6' N/7°53'26.4' E) is located sheltered in the north-east yacht harbour of Helgoland **Figure 4**, **Table 1**, considered a nearshore system. Of advantage for this study site, due to the sheltered and land-based location of *System B,* was that sampling was not contingent on harsh environmental factors e.g. waves and currents, thus regular sampling was ensured.

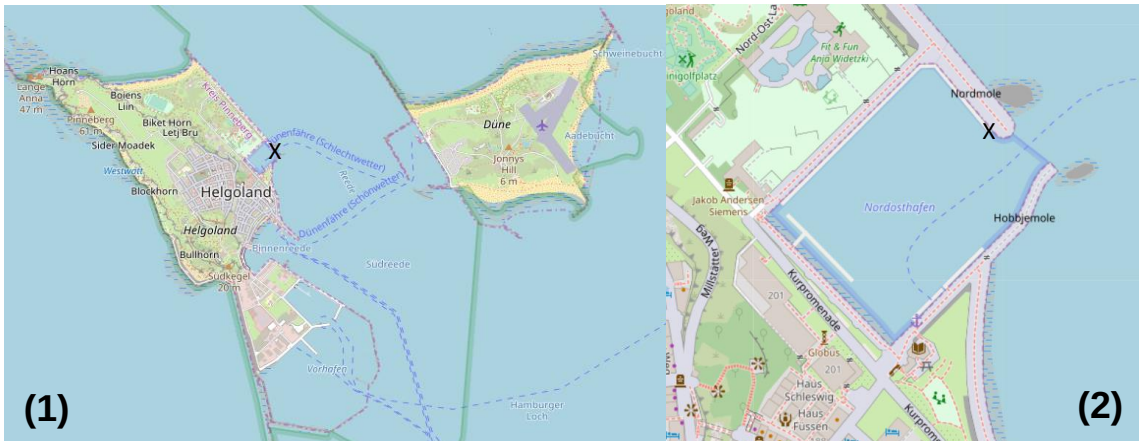

Figure 4 Map of Helgoland and *Dune* **(1)**. Detail of the north-east yacht harbour **(2)** (X) indicates the location of *System B* (Hannemann 2022)

The Helgoland site is located in the centre of the German Bight and about 60 km off the German coast. It is considered one of the few hard-bottom habitats in the south-eastern part of the North Sea (Beermann & Franke 2011). Within the Helgoland area, tidal currents up to 1.0 m/s have been measured. The low tides approach the island from south-east, high tides from north to north-east (Luther 1973). During tidal change, tidal currents converge; the directions of convergence are different at the surface and at the sea floor. Tidal range varies from 2.5 m to 3 m (Luther 1973). The currents around the island are strongly influenced by the geomorphology of the surrounding sea bed, with the island's westside being most exposed, followed by *Nordreede* and *Vorhafen* (De Kluijver 1991). The maximum wave heights (0-1 m) and weak tidal currents (0.1 m/s) observed for the southern harbour of Helgoland (Beermann 2013; Buck & Buchholz 2004) can be assumed for the northeast harbour as well. A daily long-term monitoring programme (1962-2011) of the surface sea temperature (SST) around Helgoland indicated the lowest mean temperature in February/March (3-4 ˚C) and the highest mean value in August (17 ˚C) (Wiltshire et al 2015). The program exhibited the lowest mean salinity values with a minimum in April (31.2 g/kg) and maximum in December (32.7 g/kg), respectively (Wiltshire et al 2015). Due to its land-locked, semi-enclosed nature the North Sea is exposed to a disproportionally high level of climate warming, increasing the mean SST by 1.678 °C since 1962 (Beermann & Franke 2011; Wiltshire et al 2010).

Table 1 Classification of both study sites

	Study site	
	Nordergründe (Nor)	**Helgoland (Hel)**
Description	*System A = Pentagon*	*System B = MareLift*
Code	NorSub (sheltered [S] and exposed [E])	HelEu, HelSub
Distance to Coast [km]	30	60
Classification	Offshore	Nearshore
Surveyed Habitat	Sublittoral	Eulittoral, Sublittoral
Wave Exposure	Exposed	Sheltered
Sediment	Sand	Sand, Hard substrate
Temperature [°C]	-0.1 - 21.7	3.0 - 7.0
Salinity [g/kg]	25.7 - 34.3	31.2 - 32.7
Tidal Range [m]	3	2.5 - 3
Current Velocity [m/s]	0.6 - 1.5	0.49 - 1.0

2.3 Experimental design of biofouling collectors

Within the second project aim of *EnviSim4Mare*, three biofouling collectors (artificial structures) *System A, B* and an additional buoy (buoy l) with test bodies for measurement trials in the new SSWC-flume, were developed. These systems were designed and built for being moored at the study sites Nordergründe (Nor) and Helgoland (Hel) for samples and data obtained under realistic environmental and biological conditions over time. Requirements for each system and the test bodies were robustness against site specific environmental conditions **Table 1** (e.g. waves, tidal-/currents, storms) as well as allowing regular sampling while being straightforward in its handling during sampling, transport and measurement trials (Isbert et al 2022). For the present work only *System A* and *B* are described and discussed, the additional buoy l was neglected.

Stainless-steel panels were used as test bodies (in both systems *A* and *B*) acting as artificial substrate to allow colonisation of biofouling. The chosen material for the test bodies should provide similar conditions for biofouling growth on windmill foundations. In an earlier stage of the project in 2020 black steel was used as it rather resembles the material at windmills. However, the material exhibited that panels started to corrode after a short time, causing organisms to fall off and eliminating fouling for further analyses. In 2021, during the development of the biofouling collectors, stainless-steel panels were installed, since the material is non-corrosive and providing reliable results while being a liable settlement ground for fouling organisms. In addition, the size of the panels had to be selected with requirements of easy maintenance in compact RAS on land as well as equally simple handling during evaluation in the laboratory. Test bodies measure 11.5 x 13 cm, while each panel holds four holes on the outer centimetre, whereby the panels are attached to the mainboard (subunits of PE on *Pentagon* and main panel of stainless-steel on the *MareLift*) with cable ties.

2.3.1 *System A Pentagon*

System A is located in a rather exposed area and had to be developed to withstand rougher weather conditions and more severe sea states in comparison to *System B*. It also had to ensure attachment and growth of fouling communities on test bodies (steel panels) while keeping the weight of the construction in general as low as possible. It was decided to use a spar-buoy-type **Figure 5 (1)** with a large immersion depth, allowing the biofouling collector (*Pentagon*) with test bodies to be submerged at any time. The aim was to provide straightforward sampling by reaching *System A,* the *Pentagon,* with the small Research Vessel (RV*) Uthörn* (AWI) and using a small zodiac-type boat under low wave and backwater conditions **Figure 5 (2)**.

A buoy (in the following buoy ll) was rented from the local Water Shipping Agency (WSA Bremerhaven), which is responsible for deployment and management of the buoy network in the shipping waters of the Jade-Weser-area. Spar buoys are described as narrow and elongated (Clearman 1988) and can be used in a wide range of purposes, such as in marking coastal and offshore waterways or marking hazardous areas (e.g. any underwater obstacle, shallow or rocky areas). Buoys may be used for obtaining abiotic parameters by attaching data loggers (Zhang et al 2015).

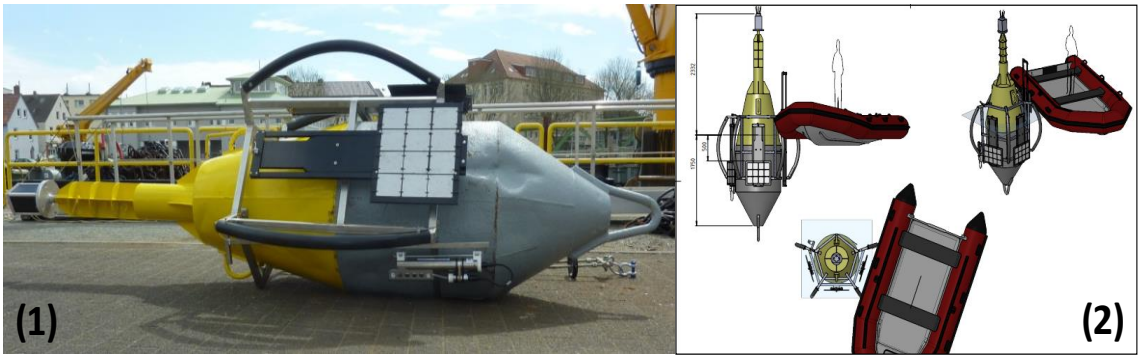

Figure 5 *System A* (*Pentagon)* attached to the spar-buoy (buoy ll) before deployment at Nordergründe site at the WSA, Bremerhaven **(1)** (picture: Isbert). Illustrated sampling procedure with a zodiac **(2)** (J. Lemburg).

The chosen buoy was made out of steel and was painted with a primer coat. The height was measured 3,830 cm (top to bottom), while about 1,750 cm of the buoy would be submerged at all times, with a mean width of 950 cm **Figure 5**. The thickness of the steel body was estimated to 8 mm with a total weight of approximately 900 kg. The top of the buoy was equipped with a radar reflector, a yellow top mark and two welded eyelets on both sides were attached, for deployment and lifting of the buoy.

The *Pentagon* **Figure 6 (1-2)** was developed by the AWI scientific workshop consisting of three mainboards made of synthetic material (polyethylene, PE) being attached to a stainless-steel frame via a slide system. Each of the boards contains 12 test bodies (stainless-steel panels) in three rows for biological monitoring of the biofouling communities. For protection of the panels from floating objects (e.g. flotsam or boats) and during sampling, the steel frame was equipped with a *crash cage* **Figure 6 (1)**.

The weight of the construction with removable main boards and test bodies is about 75 kg. The *Pentagon* was mounted around the buoy from above and a belt **Figure 6 (2)** was screwed on at the bottom. At the top of the frame a steel part (triangle) was screwed to

close the construction and finalize the attachment to buoy ll. The frame cannot not slip off over the buoy as the *Pentagon* is tighter at the top and additionally it is hold by the belt. Screwing the steel triangle to the top also prevents it from sliding up over the eyelets under rough sea conditions. During the sampling procedure on the zodiac **Figure 5 (2)** each mainboard was removed at a time from the frame and reinserted afterwards into the sliding system.

Figure 6 *System A (Pentagon)* (designed by J. Lemburg). Front view **(1)** the yellow arrow indicates the *crash cage* mounted on the steel-frame. The white arrow indicates the mainboards (black), holding the test bodies (steel-panels). View from behind **(2)** red arrow indicates the belt for attachment to buoy ll (Images: Lemburg).

2.3.2 *System B MareLift*

Since *System B,* the *MareLift,* is located sheltered in a harbour, fierce conditions such as strong waves and currents can be considered less pronounced than for *System A.* Functionality of the construction and components had to be ensured despite the sheltered location with less severe conditions. This applies also to an appropriate design for biofouling collection and straightforward handling with less personnel. The design is based in a vertical structure, additionally the aim was to permit potential installations of the system into different marine environments for future research.

The *MareLift* was mounted at the quay wall of the north-east yacht harbour of Helgoland in March 2021 (depth range 3.6-4.2 m) close to the marina exit **Figure 4 (1, 2)**. The stainless-steel girder **Figure 7 (3)** (overall length: 7,355 mm; overall width: 160 mm; 130 kg) forms the base of the construction.

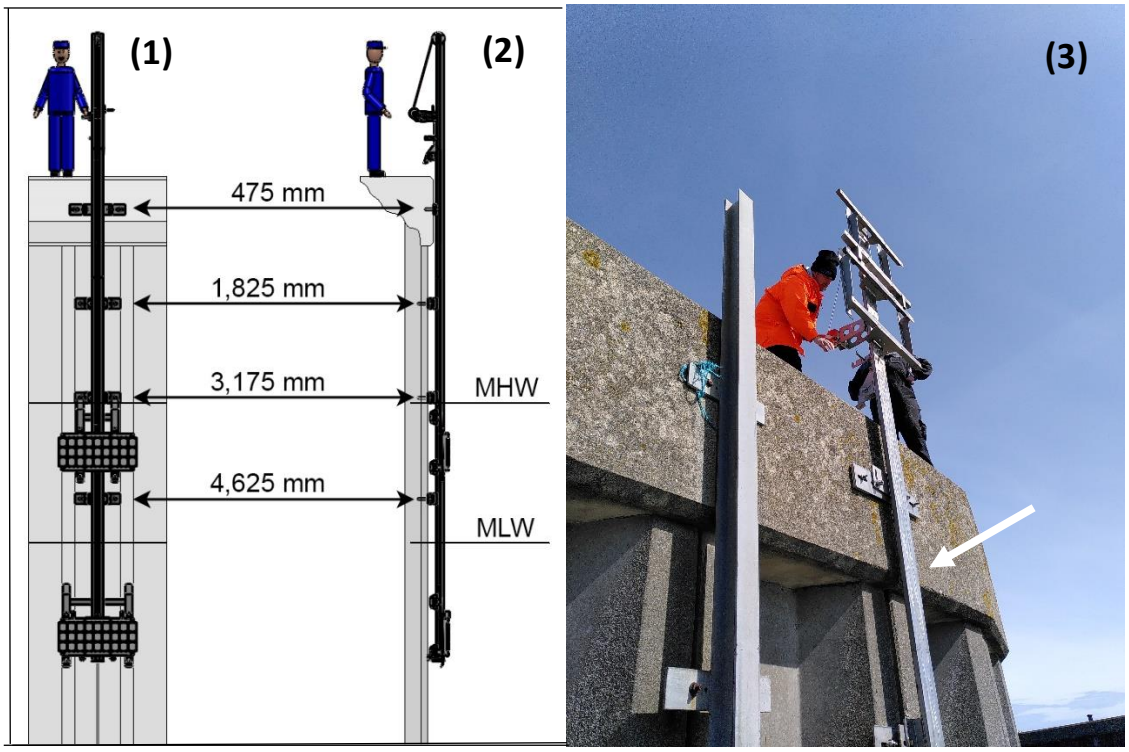

Figure 7 *System B* (*MareLift* scale 1:10) (drawing: M. Littmann, Isbert et al 2022). The scheme shows the frontal view **(1),** side view **(2). (1)** Details of girder fixation: Four flat bars doweled to the quay wall (black numbers in mm indicate distance of flat bars to the quay edge from above: First: one piece: 800 x 150 x 10 mm; second to fourth: (two pieces: 380 x 150 x 10 mm (upper part), 650 x 150 x 10 mm (lower part)). Counterparts welded on the girder: first: 265 x 150 x 10 mm, second to fourth: 420 x 150 x 10 mm, fixed with. MHW – mean high water, MLW – mean low water **(3)** Sledges in position for sampling from the quay wall without mainboards and panels the tiltable arm is not turned over. The white arrow indicates the girder (picture: Isbert).

The tiltable arm **Figure 8 (1)** (L: 1,700 mm; W: 160 mm; 28 kg) consist of two parts made of stainless-elbow-steel welded on both sides of a square tube. It was constructed to the girder for turning over the panels with biofouling for straightforward sampling. It was decided to use stainless-elbow-steel for the whole construction including test bodies due to its non-corrosive characteristics.

To attach the final construction to the quay wall, four flat bars were doweled with their lower part into the wall, using epoxy resin and two anchor rods. Girder and tiltable arm are connected by a steel hinge **Figure 8 (1)**, carrying the test bodies on two mainboards

Figure 8 (2) when lifted. The mainboards are attached to two sledges, pulled up by means of a winch, operated from the quay wall **Figure 8 (2)**. The upper sledge was located in the eulittoral (intertidal) zone, being exposed to the air in 12-hours cycles. The lower sledge was permanently submerged in the sublittoral (subtidal) zone to monitor the development of fouling communities from both habitats. The total weight of the whole construction is 296 kg.

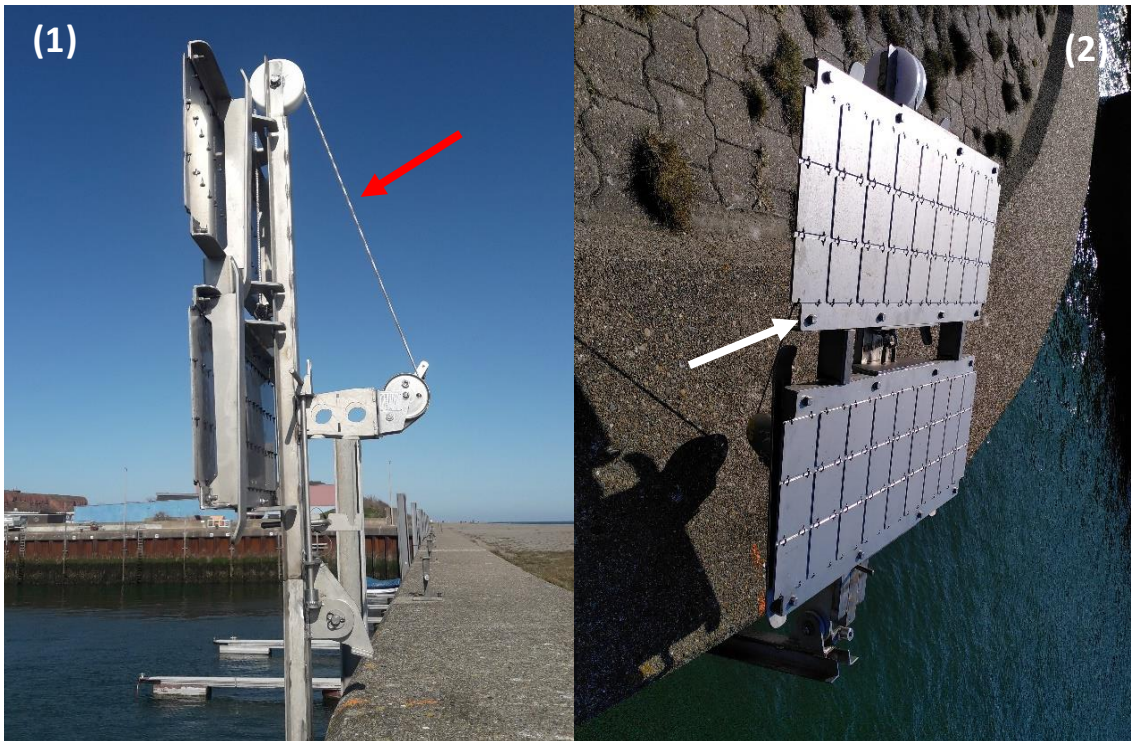

Figure 8 *System B* (*MareLift)* pulled up for the sampling procedure **(1)**, red arrow indicates the steel cable, used by the winch to pull up the sledges. The tiltable arm turned over for the sampling of the test bodies **(2)**, the white arrow indicates the mainboards with panels (both stainless-steel) (pictures: Isbert).

2.4 Growth monitoring

2.4.1 Sampling procedure at both sites

For obtaining an insight in the development of fouling communities on the deployed biofouling collectors, sampling was done monthly over two years at intervals of 4-5 weeks for both sides. The two mainboards attached to *System A* (NorSub) were constantly exposed to the tidal current, while the third mainboard with panels lied sheltered from the current behind the buoy body. Consequently, the samplings in 2021 showed that the organisms were not exposed to the same conditions on each side of buoy II. This aspect has been taken into account during both sampling and subsequent analysis in 2022.

Three panels were sampled each month at the Nordergründe site, six panels were sampled from *System B* (Hel), while three panels were taken from each habitat (eulittoral and sublittoral). For each sampling at both sites, three panels were taken vertically below each other and coded with coloured cable ties for the sublittoral: blue- top, red- middle, yellow- bottom. Additionally, for *System B* (HelEu) the three panels were sampled and coded equally in the eulittoral but with added black cable ties. During each sampling, the panels were taken from top to bottom to identify any potential differences over the slight depth difference on the mainboard. Since the panels could not be examined directly on site, they had to be prepared for further transport, with each panel being packed in a polyester gaze bag. If any organic material should have fallen off, it was assignable to each individual panel. Subsequently, the bags with panels were fixed in a cooling box into an appropriate stainless-steel device with seawater and ventilation equipment[6] and transferred back to Bremerhaven. The samples were stored in a RAS facility (located at the ZAF in Bremerhaven) at the AWI with adapted temperature and ventilation until the next day of further evaluation.

2.4.2 Morpho-taxonomic analysis of detected biofouling organisms

Further work was done with living biofouling organisms under laboratory conditions at the AWI. Each panel was placed in a tray with salt water where the current condition of the test bodies was recorded photographically with a digital reflex camera (Canon EOS 5D Mark lll) in a standardized manner from a distance of 53 cm, ensured by a reprographic stand. This served as a basis for later estimation of coverage, but also to mark specific organisms on a printed photo during sample evaluation. Under a field of 9.5 x 11 cm each panel was then examined under a stereomicroscope (Zeiss Stand K MAT and Zeiss Stemi DV4/DR). The outer edge (one centimetre) of the test bodies was not considered in the evaluation, since it might have been touched or damaged during the sampling procedure on site and did not provide representative results. All sessile species and their individuals were counted and recorded in a protocol along with an assessment of each genus' fouling rate (coverage). Living organisms were taxonomically identified to the lowest taxonomic level (genus) possible. Vagile species were recorded as well, but not included in the coverage estimations, as assigning these species to a specific panel was rather complex due to their movement behaviour and the potential loss during sampling in the field. As succession and development progressed and the number of individuals increased on the panels, individual subsamples had to be examined to minimize potential errors in assessing total abundances. For this purpose,

[6] Supply of fresh air for organisms

panel areas of 3 x 3 cm or 5 x 5 cm were analyzed. The dimensions were chosen individually according to the appearance of overall growth on the panel. This was mainly dependent on the distribution of a certain species, its abundance and size of individuals. Subsequently, the determined number of organisms was extrapolated to the area relevant for the evaluation (9.5 x 11 cm).

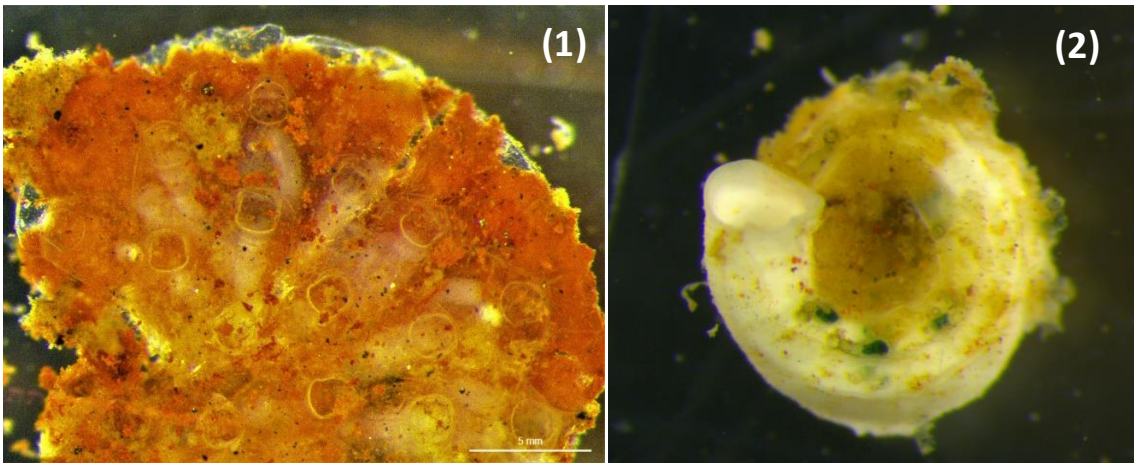

Figure 9 Example of taxonomic identification using Leica TL3000 Ergo **(1)** Bryozoa *Cryptosula* spp. **(2)** Polychaeta *Janua heterostropha* (Montagu 1803).

This method was often used for instance in the summer months of sampling *System B* (HelSub), where the abundance of certain organisms (e.g. Serpulidae) increased rapidly, whereby the subsampling facilitated the counting process for that species. In the late summer and fall months the evaluations of *System A* (NorSub) samples were partially performed with 5 x 5 cm areas in the center of each panel. More abundant individuals, especially amphipod tubes and barnacles, were recorded, counted, and evaluated within this area only. Species that were easier to count based on their size (e.g. blue mussel *Mytilus edulis,* Linnaeus 1758) were counted throughout the entire panel.

For further taxonomic identification, samples were preserved in 70 % ethanol solution and relevant literature (e.g., Handbook of the Marine Fauna of North-West Europe, Peter J. Hayward and John S. Ryland, print publication date: 2017; A Student's Guide to the Seashore, J. D. Fish, University of Wales, Aberystwyth, S. Fish, University of Wales, Aberystwyth, print publication year: 2011) was consulted. Further morpho-taxonomic analysis was performed using a binocular (Leica TL3000 Ergo) **Figure 9** and a microscope (Zeiss Axioplan 2 Imaging Fluorescence). The last step of the panel analysis consisted of scraping off the entire growth excluding the outer centimetre from the panel, weighing the biomass and deep-freezing the samples. Prior to weighing, each scratch

sample was placed on filter paper for one minute to ensure approximate equal water weight. These samples were used later to determine the biomass fraction of the fouling communities by dehydration (dry weight) and incineration (ash weight).

2.4.3 Total coverage analysis using *ImageJ*

Since the percentage of growth on the panels was initially only estimated with the naked eye, the program *ImageJ* 1.53c (Java 1.8.0_172) [Software] Wayne Rasband) was used to quantify the coverage percentage on each panel. Panels with an estimated coverage of 100 % were not further analyzed, accurate estimation was assumed. Processing with *ImageJ* would lead to incorrect results in some cases, as the fouling partially emerged from the water due to its thickness. The resulting reflections were identified as bright, in this case bare areas, by the program. Using *ImageJ*, the previously acquired images (Figure 20-24 Annex) of each panel were cropped to the format of the examined panel section **Figure 10 (1)** of 9.5 x 11 cm and converted into an 8-bit gray image **Figure 10 (2)**.

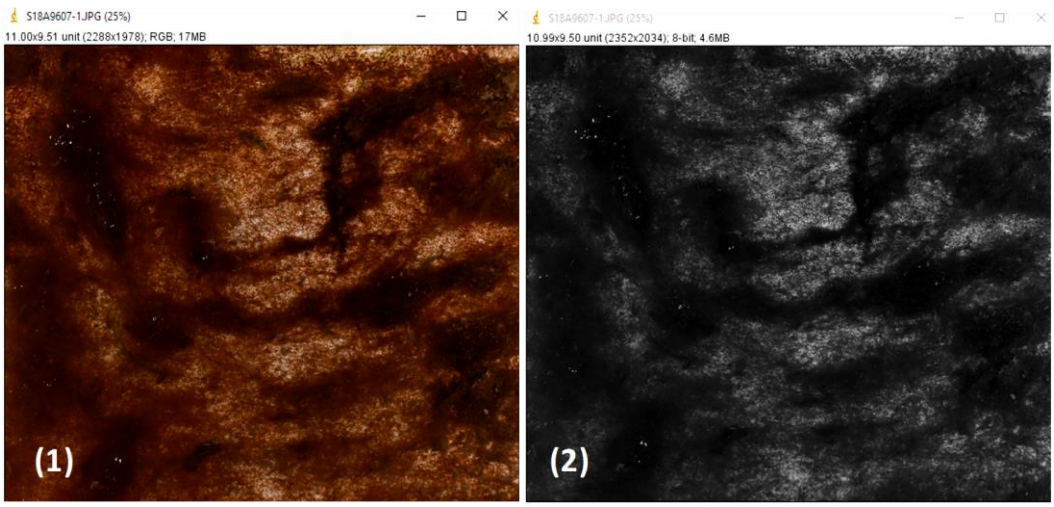

Figure 10: Examined panel section cropped to 9.5 x 11 cm (example panel: code CDMa22H, covered mostly by brown algae) **(1)** using *ImageJ*. The panel section converted into 8-bit grey image **(2)**.

The command *Image-Adjust-Auto Threshold* was then used to convert the images into binary images, with the blank panel appearing white and the fouling appearing black **Figure 11 (1-2)**. The command *Auto Threshold* provided a direct comparison of all possible *Threshold* methods **Figure 11 (1)**. In direct comparison, the method *Triangle* proved to be the most reliable, as it provided an equivalent result for all images.

The program then calculated the percentage of the black area, which resulted in the total cover **Figure 11 (2)**. This standardized and automated process was applied to all images with a fouling rate below 100 %.

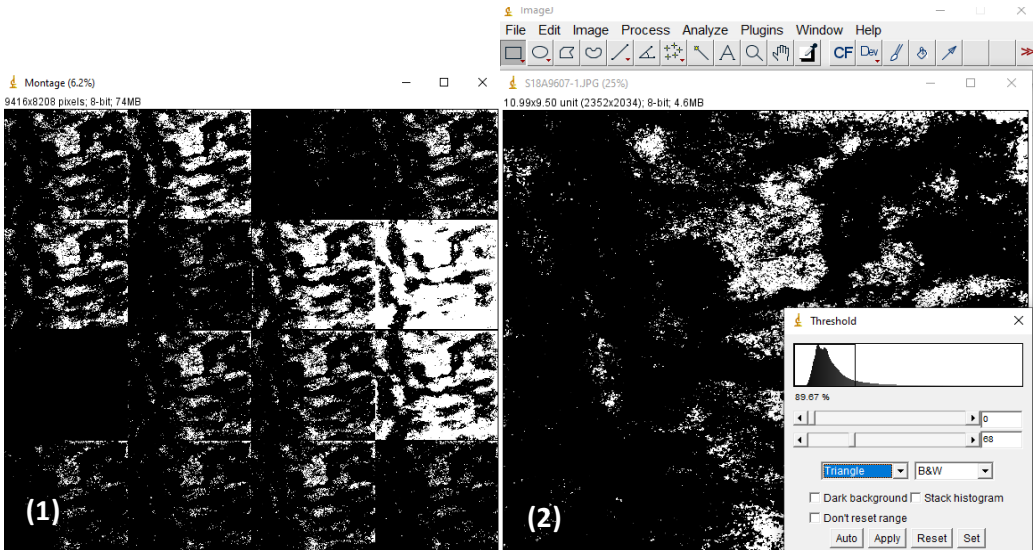

Figure 11 Command *Auto Threshold* **(1).** Coverage estimated by *ImageJ*, using *Threshold Triangle* with a calculated coverage of 89.67 % for panel CDMa22H **(2)**.

3 Results

The main focus of this work lies in the development and technical functionality of the biofouling collectors *System A* and *B* which includes the mooring and deployment as well as the handling during sample procedures. Therefore, the mooring and deployment will be included in the results section to provide this technical part in the following discussion. Since the *EnviSim4Mare* project is an ongoing project where new data is constantly obtained, certain work has not yet been completed (e.g. exact taxonomic determination of biofouling organisms). Therefore, the time period of this thesis was limited to the results and data obtained to date.

Due to logistical issues no sampling could be done at the Nordergründe site after July 2022, since no vessel was available in August. At the beginning of September 2022, *System A* on buoy ll was no longer on site and was probably lost in the end of August and the first week of September. It is suspected that a strong external force (e.g. fishing vessel/crab trawler) might be responsible for the damage, since weather conditions could be excluded as no storm and swell were recorded for that time span. Additionally, in March of 2022, after buoy ll survived heavy storms in February (three in five days), both the anchor chain and the shackles have been replaced, as a precaution measure. Buoy ll and the attached *System A* could be recovered in October and were brought back to the WSA in Bremerhaven for cleaning, retreating and preparation for anew deployment in early spring of 2023.

3.1 Deployment and handling of systems during sampling procedure

3.1.1 *System A Pentagon*

System A (*Pentagon)* attached to buoy ll was moored north-eastern of the wind farm *Nordergründe* by the WSA Bremerhaven in May of 2021. It was deployed by a buoy-laying-vessel (MS *Nordergründe*) approximately 1 nm outside of the buffer zone of the wind farm and approximately 7 nm off the northeastern coast of Lower Saxony **Figure 3 Figure 12 (1)**. Buoy ll was moored at about 11 m depth with an anchor chain (link diameter 26 mm) of 30 m length and an anchor block (concrete 3 t) **Figure 12 (2)**. The mooring was done without any difficulties.

Due to first test sampling trials on the additional buoy (buoy l), which was deployed at the Nordergründe site in April 2020, a known main challenge was the handling of the buoy owing specifically to strong tidal currents on site. Therefore, samplings at *System A* were done during the turning point of the tides only, in order to avoid movement either way in the tidal currents, and under good weather conditions (waves < 0.6 m, wind < 3

Bft). Additionally, lifting the whole construction with the lifting arc of the RV *Uthörn* was not possible due to the buoy weight, therefore a zodiac was used for sampling **Figure 12 (3)**.

Figure 12 *System A* on buoy II lifted by the crane at the Nordergründe site **(1)**. Buoy II moored **(2)** (picture: MS *Nordergründe*, WSA). Sampling procedure on the zodiac **(3)** (picture: Dechant)

Handling of the *Pentagon*'s mainboards during the first sampling trials was done straightforward and without any major difficulties. As succession on the construction increased with the summer months it became more difficult to reinsert each mainboard, due to fouling on the lower parts of the slide system. *System A* provided excellent attachment and growth of biofouling on the test bodies without loss of fouling due to corrosion while fouling communities exhibited clear successional patterns over time.

3.1.2 *System B MareLift*

The installation of *System B* (*MareLift*) in March 2021 in the north-east harbour of Helgoland was done with the assistance of a wheel loader and a forklift which enabled the fixation of the girder to the four prepared flat bars to the quay wall. Followed sampling collections in 2021 and 2022 proved that all components (sledges, tiltable arm, crank) of the *MareLift* worked perfectly and no failures were detected in both years. None of the construction parts had to be adjusted or repaired and the material exhibited almost no signs of wears or corrosion. The test bodies (stainless-steel panels) proved to be a suitable settlement and growth substrate for fouling organisms and showed no sign of corrosion provoking potential loss of biofouling. The lift could be handled very well therefore, samplings could be conducted by two persons only. Though, the overall weight of the tiltable arm (ca. 109 kg; incl. sledges, test bodies without potential biofouling

weight) required a certain effort even for two persons when turning over for sampling or placing the arm in the upright position.

3.1.3 Environmental conditions at both study sites

To evaluate environmental conditions in regards to construction functionality of both systems and development and growth of fouling community composition at both study sites, more accurate data was required. The abiotic data were provided by the BSH (Brüning 2021). However, it must be mentioned that the data is based on model calculations instead of measured values, the data is used for later subsequent forecasts. The calculations are based on the BSH-HBMnoku circulation model, in which biochemical properties of coastal waters are coupled with a hydrodynamic circulation model to obtain more accurate values. The data are obtained in several model runs per day and are transferrable to any coordinates in German coastal waters, but inaccuracy of the projections may increase with vicinity to the coast (Brüning 2021).

Additionally, a HOBO data logger was installed in the eulittoral (August 2021) and the sublittoral (December 2021) of *System B* (Hel) to monitor local differences between these habitats.

Due to logistical issues, no data could be calculated further until July 2022 for the Nordergründe site. Additionally, salinity and temperature data for the Helgoland site could not be calculated by the BSH in 2022. The HOBO data logger was therefore used to obtain temperature data for the Helgoland site in 2022.

Current velocity

Current values were calculated by the BSH from January 2021 to July 2022 in one meter depth **Figure 13**. The eastward and northward directed currents for both study sites were differentiated and mean values for both study sites were determined. The standard deviation (SD) for the current mean values were calculated quite high for both study sites, hence for reasons of simplicity and clarity a descriptive plotting is presented without SD (Table 3 Annex) of the average velocities.

The offshore study site Nordergründe showed, in contrast to the sheltered Helgoland study site, higher average current velocities, due to the different exposed locations. On average in 2021 (January to December), the mean eastern current velocity of the Nordergründe site was calculated 0.62 ± 0.31 m/s, the mean northern current velocity average was 0.54 ± 0.26 m/s **Figure 13**. On average in 2022 (January to July), the eastern current speed velocity of the Nordergründe site was calculated 0.54 ± 0.20 m/s, the northern current velocity average was 0.44 ± 0.26 m/s.

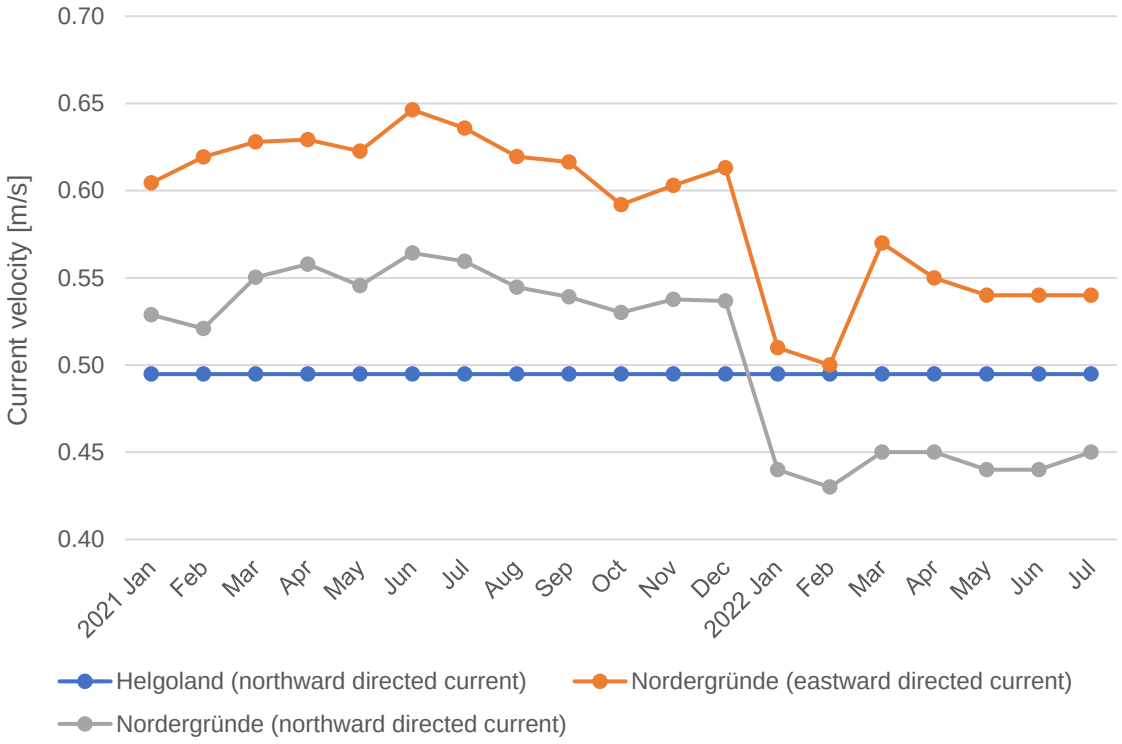

Figure 13 Mean velocity of northward and eastward directed currents [m/s] for the Nordergründe and Helgoland study sites calculated from January 2021 to July 2022 in 1 m depth (Brüning et al 2022). The calculated standard deviation (± SD) for mean current values were determined quite high for both study sites, for reasons of simplicity and clarity a descriptive plotting is presented without SD of the average velocities.

The eastward directed current of the Helgoland site was calculated in 0 m/s presumably owing to the sheltered location of *System B* and was therefore neglected in the plot. The Helgoland site exhibited a consistent average northward directed current velocity of 0.49 ± 0.29 m/s throughout 2021. A consistent average current velocity of 0.49 ± 0.29 m/s throughout the months of 2022 was calculated for the Helgoland site in 2022 as well **Figure 13**.

Water temperature

The direct comparison of both study sites showed a similar trend in the average water temperature at a depth of one meter from January to December 2021 (Nor 10.58 ± 6.07 °C, Hel 10.55 ± 5.07 °C) **Figure 14**. For the Nordergründe site more distinct variation of maxima and minima temperature throughout both years were observed. For the Helgoland site (Jan-Oct) an average annual average of 11.73 ± 4.61 °C was recorded in 2022.

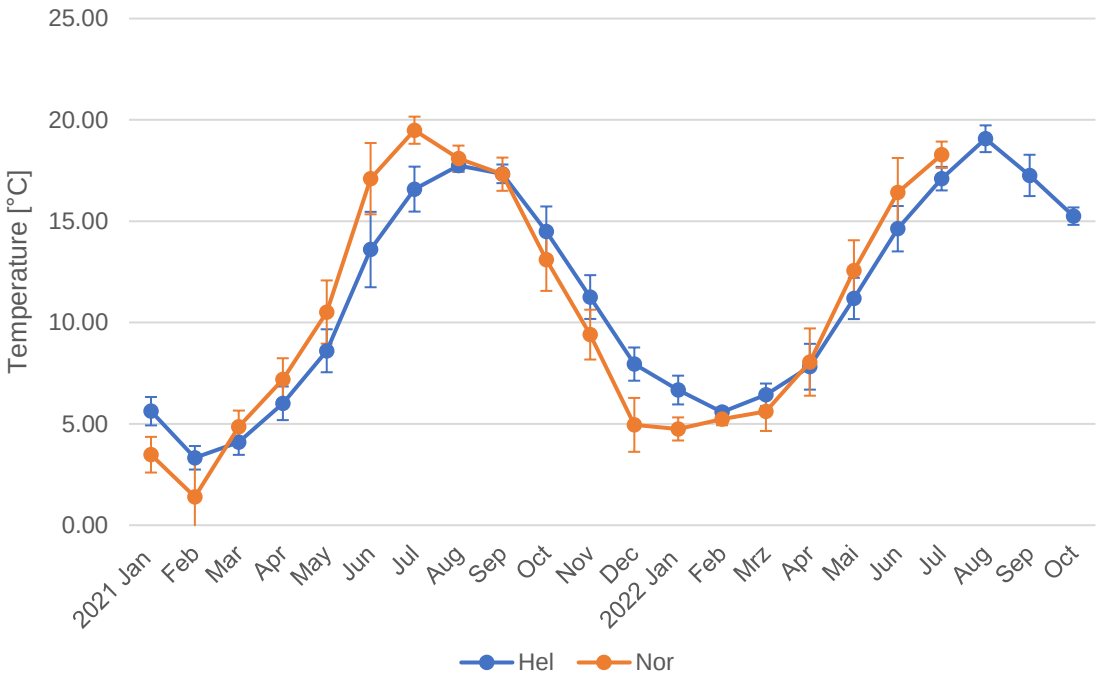

Figure 14 Mean water temperature ± SD [°C] for a depth of 1 m of both study sites Nordergründe (Jan 2021-July 2022) (Brüning et al 2022) and Helgoland (Jan-Dec 2021 Brüning et al 2022 and Jan-Dec 2022 HOBO).

HOBO data logger water temperature

Temperature measurements were taken every half hour with the HOBO data logger at the Helgoland site and mean temperatures were plotted per month from August 2021 to October 2022 **Figure 15**. Wider temperature differences were recorded for the eulittoral since the logger was submerged during the high tide and exposed during the low tide, resulting in higher SD. An average annual temperature of 13.23 ± 4.85 °C was calculated in the eulittoral (August 2021-October 2022). In the beginning of December 2021 an additional HOBO data logger was installed in the sublittoral of *System B* (Hel). For the sublittoral an average annual temperature of 11.73 ± 4.61 °C was calculated (December 2021-October 2022).

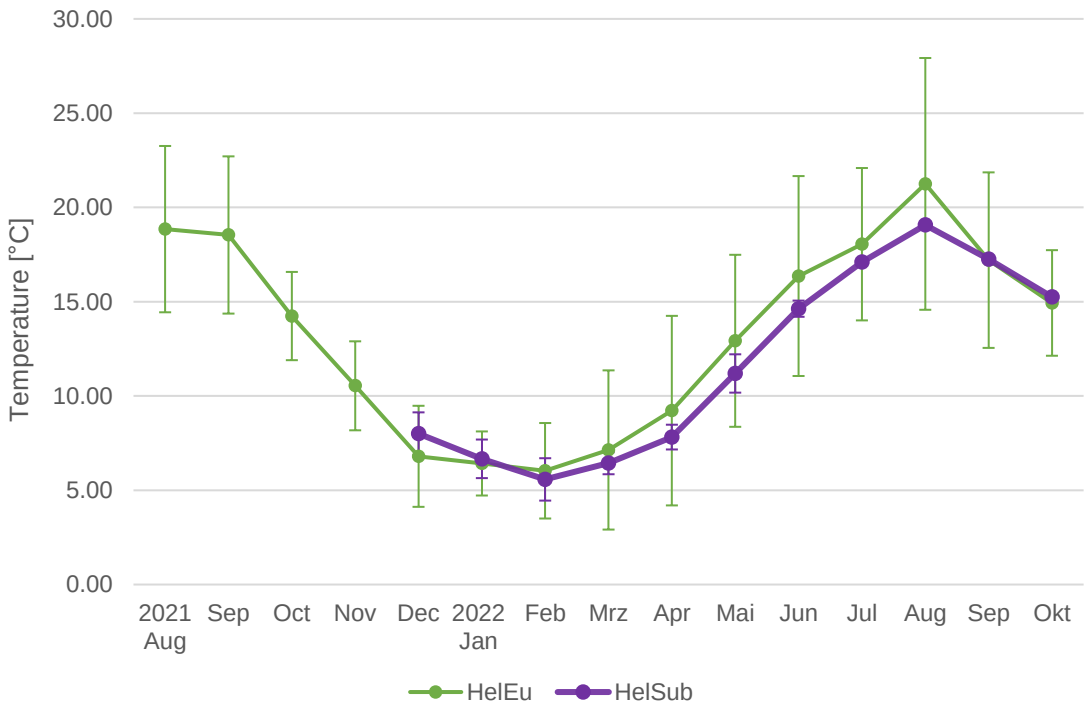

Figure 15 Mean measured water temperature ± SD of the tidal zone, HelEu (Aug 2021-Oct 2022) and the sublittoral HelSub (Dec 2021-Oct 2022) zone at *System B* using the HOBO data logger.

Salinity

The mean salinity value of the Nordergründe site was calculated lower and exhibited more distinct variations of maxima and minima, resulting in higher monthly deviations **Figure 16**, with an average of 30.91 ± 1.17 g/kg (Jan-Dec 2021). Additionally, the mean salinity value for the Nordergründe site in 2022 (Jan-Jul) was calculated 32.15 ± 0.82 g/kg and showed overall that this site was under a great influence of the Weser estuary (fresh water input), whereby salinity levels fluctuated majorly. The Helgoland study site was characterized by a significantly more stable salinity, with a mean annual value of 33.13 ± 0.66 g/kg (Jan-Dec 2021). Both sites showed a slight increase in salinity in the winter months.

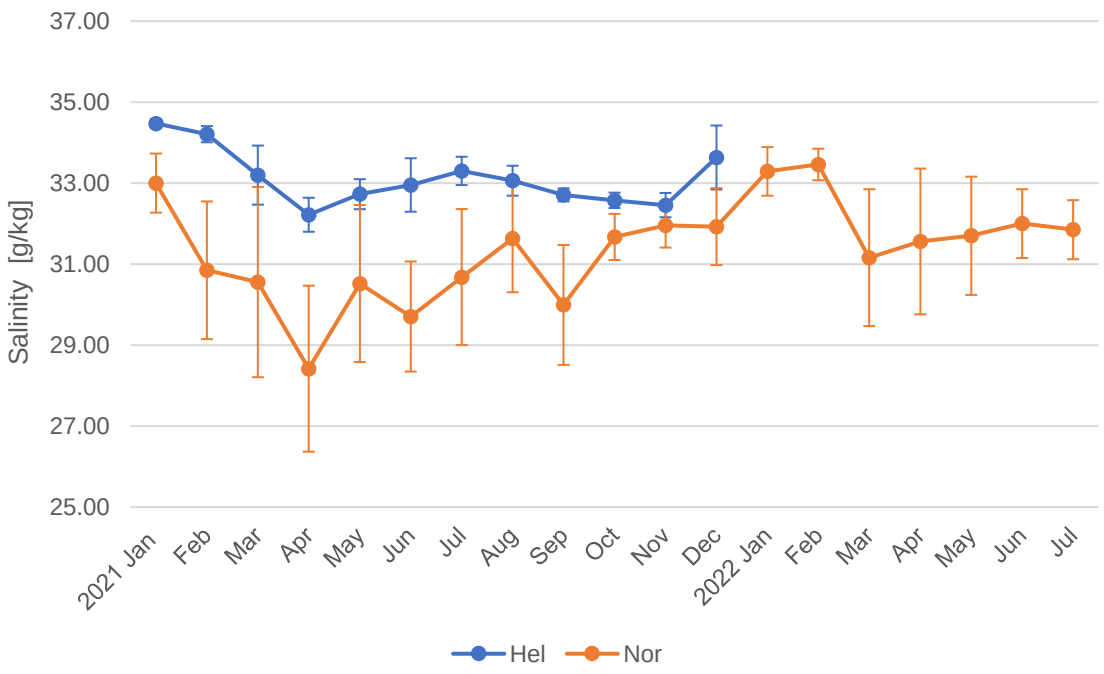

Figure 16 Mean salinity values ± SD [g/kg] in one meter depth for Nordergründe (Jan 2021-Jul 2022) and Helgoland (Jan-Dec 2021) (Brüning et al 2022).

3.2 General development of sessile biofouling taxa on test bodies

Sampling was done on a monthly basis; *System A* (Nor) in 2021 from May-November, in 2022 from April-July; *System B* (Hel) in 2021 from April-December and 2022 from April-October. Due to severe weather conditions and resultant logistical constrains no sampling was done in October 2021 at both sites. Overall, 111 panels (57 in 2021, 54 in 2022) were sampled, photographed and evaluated within both years and study sites. For the Nordergründe site 15 panels were examined in the first year, 12 panels in the second year. For the Helgoland site 42 panels were evaluated in each year, 21 panels in the eulittoral, 21 in the sublittoral**.** An increase of general coverage in biofouling on the test bodies over time was recorded in both study sites (Hel and Nor) and in all three habitats (HelEu, HelSub, NorSub).

For reasons of simplicity and clarity a descriptive plotting is presented with the percentages the dominating taxa in each habitat, month and both years **Figure 17**. In general, panels sampled in the spring and early summer months showed an average low fouling rate and plenty of bare space. The fouling coverage increased rapidly in the late summer months on all panels and stagnated mostly throughout early to mid-fall months. An average decrease in early winter months (2021) was noticeable.

Considering the samplings at the sublittoral of the Nordergründe (NorSub21) site, the early summer months in 2021 showed a clear distribution of brown algae, juvenile barnacles, hydrozoans and very few blue mussels *M. edulis*, whereby the barnacles clearly dominated the fouling community within the first sampling trials **Figure 17**. In July and August an increasing in amphipod tubes of the tube building genus *Jassa* (Leach 1814) was perceptible, whereas *M. edulis* increased as well, overgrowing the underlying barnacles. Amphipoda (81.7 ± 15.46 %) dominated in September as barnacles and the blue mussel decreased, which seemed to shift in November with blue mussels as dominating taxon (95 %) on all panels as they grew in size, barnacles and amphipoda abundances decreased notably. In 2022 sampling trials started in April, two months earlier. Additionally, after the experiences of the year before, two different conditions (sheltered and exposed) on *System A* were considered during sampling and evaluation (see above 2.4.1). However, brown algae were the dominating taxa (79 ± 7.47 %) in April as well, followed by a small coverage of barnacles and juvenile *M. edulis.* This shifted rapidly in May, where barnacles (41.3 ± 22.87 %) were dominating the fouling community, followed by blue mussels and few brown algae. A rapid increase of amphipoda tubes was observed in June followed by a decrease in July, where the proportion of both *M. edulis* and barnacles was quite even.

The Helgoland habitats (HelEu, HelSub) showed extended blank areas on all panels within the first three months of sampling (2021: May-July, 2022: April-June), especially HelEu panels were almost blank within the first two months **Figure 17**. An increase of fouling was noticeable in August 2021 and July 2022 in the sublittoral habitat of Helgoland, whereby the successional pattern in both years appeared quite similar.

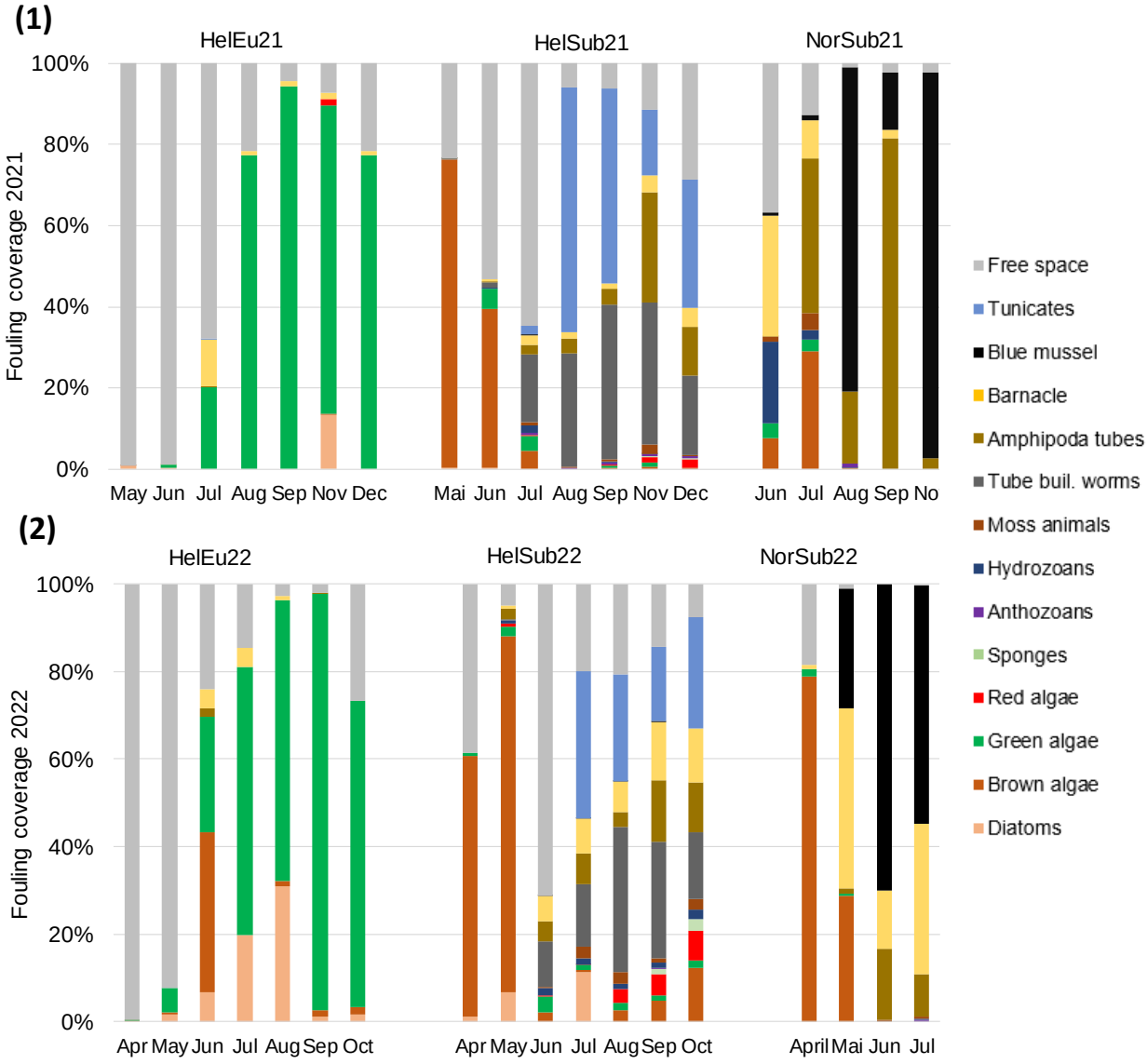

Figure 17 Mean monthly fouling coverage [%] of all habitats in 2021 **(1)** and 2022 **(2)** for each sampling month.

The Helgoland eulittoral habitat coverage of the panels was mostly dominated by green algae throughout the whole year and appeared similar in their phenology in both years as well.

The sublittoral (HelSub) panels, previously dominated mostly by brown algae, exhibited a decrease in algal growth in the early summer months of both years (July 2021/June 2022). On these panels a rapid increase of fouling was monitored in the following summer, fall and early winter months (August-December in 2021, July-October 2022). Calcareous tubeworms (Class Polychaeta), various sea squirts (Class Ascidiacea) and amphipoda (Class Malacostraca) tubes were dominating the fouling community with decreasing blank areas in regards to the fall and early winter months in both years.
Overall, the seasonal succession pattern of the detected taxa appears quite similar in the phenology of biofouling over both years and all three habitats, considered sampling started earlier in 2022. The thickness of biofouling was detected majorly thicker in Nordergründe than Helgoland due to immense layering of barnacles, blue mussel and amphipoda tubes throughout the year.

3.2.1 Morpho-taxonomic analysis of detected biofouling organisms

A total of 76 taxa were identified on all panels and both years **Table 2**. Seventeen of those taxa occurred at both study sites, 6 taxa were found in all three habitats in 2021 and 2022. In the NorSub habitat thirteen taxa were detected only in 2021, two taxa in 2022 and ten in both years. For the HelEu habitat six taxa were found only in 2021, twelve taxa in both years. Sixteen taxa were found only on the HelSub habitat panels in 2021, six taxa in 2022 and 27 in both years. Since not all taxa could be determined to species level, these were numbered by a roman number (e.g. Phaeophyceae Type II). Additionally, the tubes of polychaeta (Ampharetidae) and amphipoda were included in the analysis although being no living taxa, they were part of the permanent fouling coverage.

Table 2 Recorded taxa in both study sites. Code records: 1=2021, 2=2022, 12=both years

	Study site				Study site		
Taxon	**HelEu**	**Hel Sub**	**Nor Sub**	**Taxon**	**HelEu**	**Hel Sub**	**Nor Sub**
Ochrophyta				**Annelida**			
Bacillariophyta	12	12		Amphaetidae	12	12	
Algae				Amphaetidae Tubes		12	
Phaeophyceae				*Janua* sp.		12	
Phaeophyceae Type I	1	12	2	Serpulidae		2	
Phaeophyceae Type II		1		Annelida Type I			1
Phaeophyceae Type III	12	12	1	Annelida Type II	1		
Phaeophyceae Type IV			12	Annelida Type III	1	1	
Chlorophyta				Annelida Type IV		1	
Chlorophyta Type I	12	12	1	Annelida Type V			2
Chlorophyta Type II	12	12	12	*Nereis* sp.			12
Chlorophyta Type III	1	2		**Nemertea**			
Rhodophyta				Palaeonemertea		2	12
Rhodophyta Type I		12		**Plathelminthes**			
Rhodophyta Type II		12		Turbellaria	1	12	1
Rhodophyta Type III		2		**Arthropoda**			
Rhodophyta Type IV		2		Amphipoda	12	12	12
Porifera				Amphipoda Tubes		12	12
Sycon sp		1		Decapoda		12	1
Leucosolenia sp.		12		Copepoda	12	12	1
Porifera Type I		1		Isopoda	1	12	
Porifera Type II		12		Balanidae	12	12	12
Porifera Type III		12		*Semibalanus balanoides*		1	1
Cnidaria				*Balanus balanus*			1
Anthozoa Type I		12		Tanaidacea		12	
Anthozoa Type II		1		*Caprella* sp.		1	
Anthozoa Type III			12	Acari Type I	12	1	
Metridium senile		1		Acari Type II	12		
Tubulariidae Type I		1	12	Chironomidae Larvae	12		
Hydroza Campanulariidae		1	1	**Mollusca**			
Hydrozoa Type I		12		*Mytilus edulis*		1	12
Hydrozoa Type II			1	*Lacuna* sp.		12	
Hydrozoa Type III			1	Gastropoda Type I	12	1	
Ephyra Larvae		1		Gastropoda Type II		2	
Bryozoa				Nudibranchia Type I			1
Electra pilosa		12	1	Nudibranchia Type II		12	
Tricellaria inopta		12		Polyplacophora		1	
Cryptosula sp.		1		**Chordata**			
Shizoporella sp.			1	*Didemnum* sp.		12	
Scuparia sp.		1		*Botryllus* sp.		12	
Walkeria uva		12		*Ciona intestinalis*		12	
Bryozoa Type I		1		*Ascidiella scabra*		12	
Bryozoa Type II			1	Ascidiacea Type I		12	
Bryozoa Type III			1	Ascidiacea Type II		2	
Bryozoa Type IV			2	**Echinodermata**			
				Ophiuroidea		12	

3.2.2 Total coverage analysis using *ImageJ*

The percentage deviation of the fouling rates calculated using *ImageJ* compared to those determined by naked eye was -3% for NorSub21, 10% for HelEu21 and 17% for HelSub21 on an annual average. The Nordergründe site fouling rate was often estimated lower by naked eye than for the Helgoland site in the first sampling year of 2021. The annual average deviation for NorSub22 was calculated 1%, HelEu22 was calculated to -3% and for HelSub22 it was 6%. The NorSub and HelSub coverage of test bodies was slightly estimated higher with naked eye, whereas for HelEu it was estimated slightly lower in the year of 2022. Overall, the deviations of estimations with naked eye and *ImageJ* were higher in 2021 than in 2022. Due to rather small differences, the average coverage of panels A, B and C per month and both years was determined and plotted to provide a better visualization **Figure 18**. The values determined with *ImageJ* showed quite distinct spatial and seasonal differences in the cover distribution.

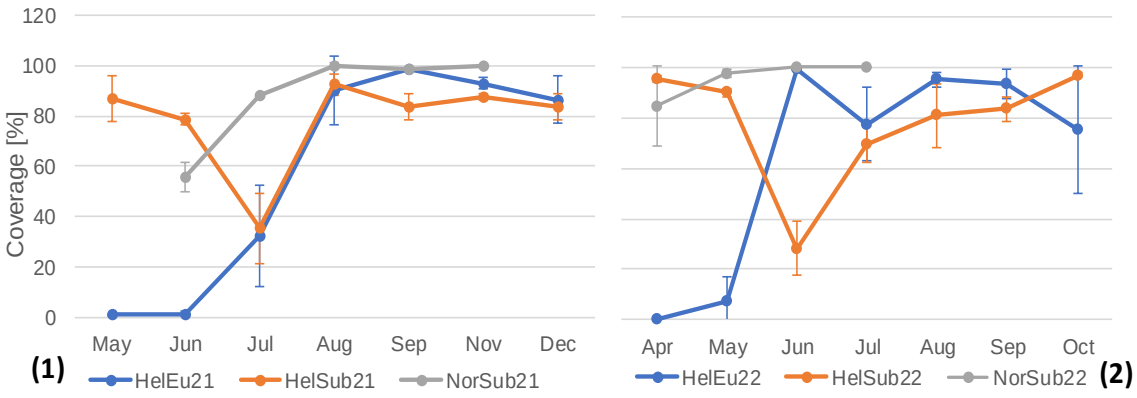

Figure 18 Mean coverage [%] ± SD of 2021 HelEu21 and HelSub21 from May to December (excluding October) and NorSub21 from June to November (excluding October) **(1)**. Mean coverage [%] ± SD of 2022 HelEu22 and HelSub22 from April to October and NorSub22 from April to July **(2)**.

For the study site NorSub21 **Figure 18 (1)** an annual average coverage of 88.65 ± 21.97 % was determined. Starting with the minimum in June of 55.83 ± 35.85 %, the coverage steadily increased to 100% in August, with panels remaining fully covered until the end of sampling trials in November 2021. The annual mean fouling rate for NorSub22 **Figure 18 (2)** was determined with 95.50 ± 10.50 %, starting with a minimum in April of 84.52 ± 16.01 %, the coverage steadily increased to 100% by June remaining until July. After one month (April 2021, June 2022) of exposure in both years the test bodies were already significantly overgrown with fouling communities with this rapid settlement pattern

monitored throughout 2021 and 2022. Even though, sampling trials started earlier in 2022, the seasonal pattern occurred quite similar in both years.

Within the first two months HelEu21 (May and Jun) and HelEu22 (Apr and May) test bodies showed the lowest coverage of the year and of all habitats **Figure 18 (1-2)**. A distinct increase to a maximum cover of 98.87 ± 0.38 % occurs from June to September in 2021, which slightly decreased in December. At HelEu22 an increase to a maximum cover of 99.06 ± 0.36 % occurred already in June, with a distinct decrease in July, followed by a slight increase in August and afterwards decreasing again until October. The annual average coverage of all panels at HelEu21 was determined 57.52 ± 42.43 %, at HelEu22 64.27 ± 41.03 %.

The annual coverage pattern of HelSub21 and HelSub22 on test bodies proceeded quite similar throughout both years. After one month (May 2021, Apr 2022 respectively) of exposure in both habitats and years the test bodies were already significantly overgrown with biofouling **Figure 18 (1-2)**. A distinct decrease of coverage was visible in both years in the early summer months (Jul 2021, Jun 2022 respectively), followed by a distinct increase over the fall and early winter (Dec 2021, Oct 2022 respectively). Average annual coverages of 78.37 ± 19.32 % for HelSub21 and 77.72 ± 23.07 % for HelSub22 were determined.

In comparison to the Nordergründe site, Helgoland site annual coverages showed more distinct variations of maxima and minima in both habitats, resulting in higher monthly deviations throughout both years and in both habitats. Whereas a full coverage of 100 % of all panels was obtained after only two months (2021) and one month (2022), respectively at the Nordergründe site. Although in 2022 sampling began two months earlier on the Nordergründe site and one month earlier at the Helgoland site, a similar seasonal pattern in coverage was evident in both years and all three habitats.

The values determined with *ImageJ* showed that individual fouling coverage on A, B and C panels do not differ much in habitat or site **Figure 19 (1-6)**, a trend for the different height of the panels on the mainboards was not recognizable in general. Coverage differences were only visible in some months and on individual panels. For example, in July HelSub21 habitat **Figure 19 (2)** panel A (31.34 %) and C (20.79 %) showed a moderate fouling rate whereas panel B (54.15 %) showed a higher determined rate.

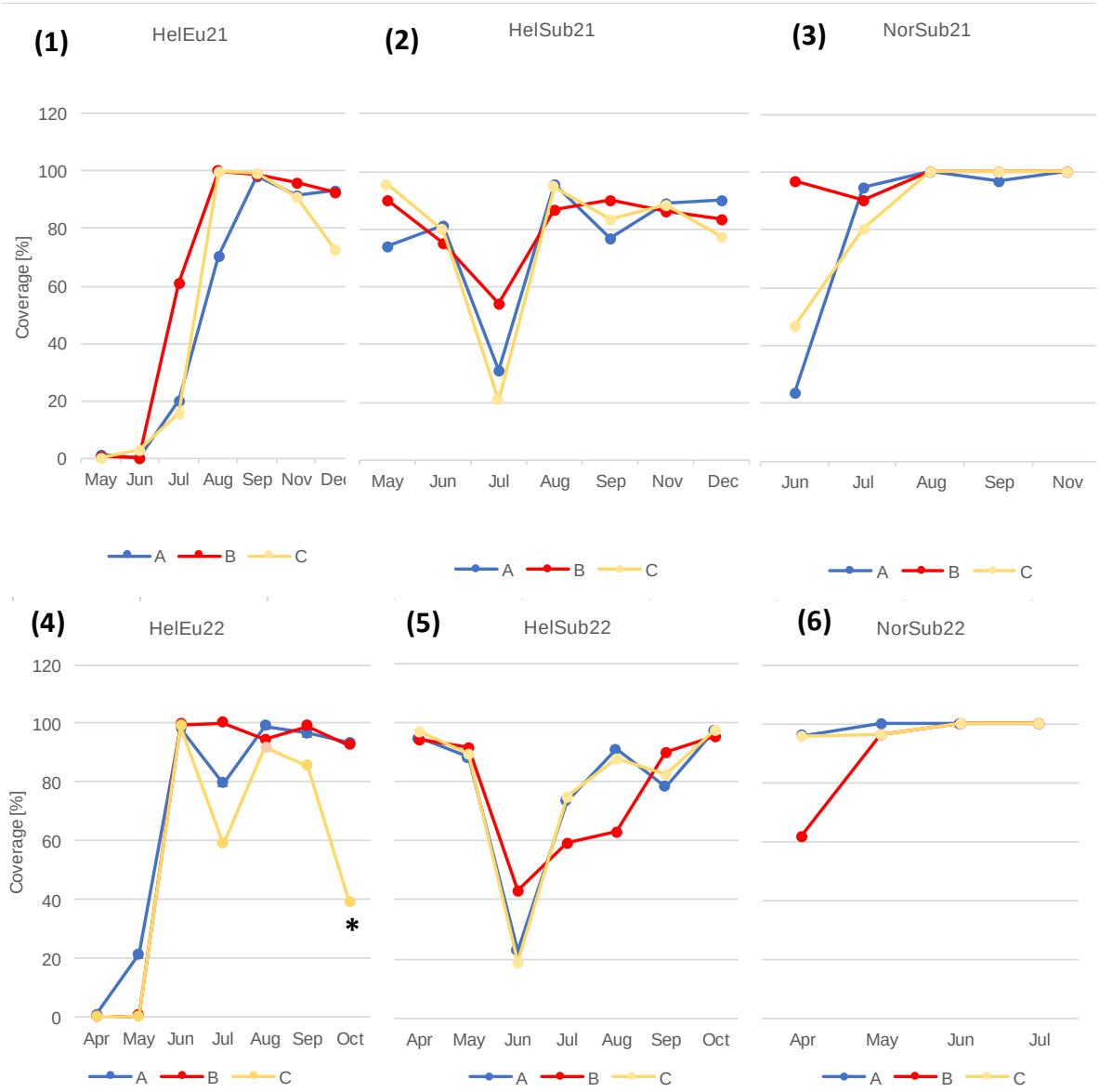

Figure 19 Coverage [%] estimated with *ImageJ* for each individual panel (A, B, C) taken in 2021 HelEu21 **(1)**, HelSub21 **(2)** from May to December (excluding Oct). NorSub21 coverage values from June to November (excluding Oct) **(3).** Coverage [%] of 2022 HelEu22. ***** Indicates the low coverage value of the C Panel, due to algae on the mainboard of the *MareLift*, scouring the fouling off the panel, resulting in a divergent coverage rate **(4)**. HelSub22 from April to October **(5)** and NorSub22 from April to June **(6)**.

4 Discussion

Technical functionality of the biofouling collectors

In general, both *Systems A* and *B* proved to be reliable collectors for biofouling communities within the sampling period of this work. Requirements of robustness towards site specific environmental conditions (e.g. waves, tidal-/currents, storms) as well as allowing straightforward handling during regular sampling procedures, transport and measurement trials, were met at both sites. The obtained data allowed a reliable basis for the assessment of spatial and temporal succession processes of biofouling communities as well as for taxonomic determination of the collected organisms.

Since *System A* withstood severe environmental conditions during the winter months of 2021/2022, robustness of the *Pentagon* construction attached to buoy ll was approved. The challenge of exposed sites such as Nordergründe is, that sampling trials are highly dependent on weather and current velocity conditions. Therefore, samplings were planned to be conducted at the turning point of the tides, which required a certain frame of forecast on date and time. Furthermore, *System A* was located at the verge of the wind farm *Nordergründe*, with other stakeholders (e.g. fishing vessels) working within this area. Latter could be the reason for the loss of the buoy and a large part of the test bodies in late summer 2022. Therefore, currently it is discussed to deploy buoy ll at a different site to avoid interaction with any fishing vessels, a final decision has not been made yet. Additionally, the accessibility of the institute RV *Uthörn* was not given at any time (schedule, shipyard time). Though, it can be stated that since in exposed study sites the opportunities of regular monitoring are often constrained due to varying marine environmental conditions (e.g. Langhamer et al 2009; Want et al 2021), *System A* offered frequent samplings for a solid monitoring basis.

System B (*MareLift*) proved the robustness and functionality for sampling procedures in a sheltered area, where it could be accessed and used regardless of the tidal and weather conditions with little personnel effort. Both different habitats (eulittoral and sublittoral) were also reflected on the test bodies providing the basis for the spatial and temporal assessment of fouling communities.

Overall, both systems *Pentagon* and *MareLift* provided excellent growth of fouling communities on all panels during both years of sampling trials, while offering simplified samplings of fouling communities in an exposed and sheltered area, respectively. The biofouling collectors can replace costly diving operations and therefore, diminishing the overall risks by operating in open waters with high current velocities and wave movement such as the Nordergründe site. Further, sheltered locations such as the north-east

harbour of Helgoland, often exhibit intense boat traffic, especially in summer months, whereby diving operations in marinas may disrupt passing vessels and risk divers.

Images (i.e. videos) are frequently used in biological monitoring trials to obtain quantitative biofouling samples on static objects (e.g. windmill foundation, buoys), often resulting in difficulties in evaluation, since visibility is not always given (e.g. plankton or sediment flow) (Orejas et al 2005). Additionally, a standardization of photographs taken by divers can be difficult to achieve especially in areas of water surfaces with strong swells and currents, as movement can cause uneven or blurred images. The obtained images in this work, in comparison, were recorded in a standardized manner, resulting in footage for comparison of all habitats and for further data processing (e.g. *ImageJ*).

The used stainless-steel panels as test bodies proved to be a proper settlement surface for fouling organisms on both sites and for all three habitats. Due to the panels size, sampling and handling could be done straightforward on site. The analysis of the test bodies under laboratory conditions offered a standardised evaluation process to conduct spatial and temporal comparisons and are therefore considered as appropriate tool for biological monitoring of fouling communities (e.g. Beermann, 2013; Menchaca et al 2014; Want et al 2021). In earlier trials of the *EnviSim4Mare* project test bodies made of black-steel were used. Due to the intense corrosion of these panels, biofouling (organic matter) was lost by falling off the panels during sampling and could not be considered in the total coverage analysis. Likewise, Want et al (2015) faced a similar issue and replaced the black-steel panels with stainless-steel panels as well. The stainless-steel panels haven been proven to be better fouling substrate, as extensive corrosion may prevent accurate assessment of biofouling (personal observations in 2020; Want et al 2015).

General biofouling development

The development of young fouling communities could be monitored in two years at the exposed and sheltered study sites, showing different seasonal and spatial succession pattern within the communities. Fast settlement and intense growth are typical characteristics in the first phase of ecological succession (Connel & Slatyer 1977; Horn 1974) and were observed in the colonization process on test bodies of both systems *A* and *B*. The studied taxa represent a variety of diverse soft- and hard-fouling organisms, which commonly colonize on artificial hard substates in the German Bight (Schröder et al 2008).

A total of 76 taxa were identified on all panels and both years, whereas 69 taxa were recorded in 2021 and 56 taxa in 2022 sampling trails. Different total numbers of taxa were recorded at both sides and all three habitats: 27 (2021) and 13 (2022) taxa on

System A (Nordergründe site) and at *System B* 18 (HelEu21), 12 (2022) and 49 (HelSub21) and 40 (2022) taxa. In the second year of the *EnviSim4Mare* project some taxa were already familiar and could be accordingly identified, whereby the total number of taxa in 2022 resulted in lower numbers. At the Nordergründe site test bodies were clearly dominated by blue mussels, associated with *Jassa* spp. and their tubes in both years. The eulittoral of the Helgoland site was dominated by filamentous *Ulva* spp. and larvae of the Chirinomidae in both years, the sublittoral was dominated by calcareous encrusting tubeworms and encrusting ascidians in both years as well.

In a study done by Kerckhof et al (2009) a total number of 49 taxa were recorded after 3.5 months studying (May-September 2008) biofouling settlement on windmill foundations off the Belgian Coast. The observed splash zone (5-0 m) was characterised by the larvae of Chirinomidae as well as in the present study (HelEu). They observed a Barnacle-*Jassa* community in the low intertidal (0-3 m). With regards of the initial settlement phase of 3.5 months, this was also observed on the Nordergründe panels. In comparison 54 species were recorded on the FINO l piles (southern German Bight) after a study period of 17 months (April 2003-December 2004; Orejas et al 2005). In depths of 2-3 m the blue *Mytilus edulis* dominated the fouling community of the piles firmly by the summer (2004; Orejas et al 2005). This was observed in the summer months of 2021 (August) and early summer of 2022 (June) in the present study as well.

In all three habitats of both sites the colonization process of the studied biofouling communities showed an expected colonization sequence of taxa as well as a seasonal succession pattern on the artificial hard substrate in both years. All panels indicated bare patches in the first sampling trials during the spring months for 4-12 weeks (depending on the habitat). Typical primary colonizers (Bacillariophyceae), followed by macroalgae spores settled on the test bodies within the first weeks of community development in both sites. With longer exposure algae appearance decreased, particularly at the Nordergründe site, and various macro-foulers started to settle. A peak of coverage was monitored in late summer of 2021 and late spring of 2022 at the Nordergründe site, where the panels were completely overgrown. During the summer months (August 2021/July 2022) a peak of fouling community coverage was noticeable in both years at the Helgoland site (both habitats), whereas some areas of stainless-steel were still uncovered. Though overall, both sites and all three habitats differed clearly in their phenology over the year.

Site-specific biofouling development

Nordergründe

In general, the composition of biofouling does not differ much in its phenology in both years of sampling at the Nordergründe site. A cold snap was observed in the winter months of 2020/2021 with lower mean temperatures (February T° 1.4 ± 1.72 °C) compared to the winter months of this year (February T° 5.24 ± 0.31 °C). This aspect may have influenced the different seasonal succession pattern observed in-between both years. The initial phase of settlement in 2021 was characterized by the colonization of brown algae, barnacles and hydroids, which was then followed rapidly by dominating tube building amphipods of the genus *Jassa* spp. and the blue mussels *M. edulis* in the summer months. The sublittoral biofouling communities at the Nordergründe site in 2022 were characterized by a pioneer settlement of brown algae and barnacles, which were rapidly overgrown by the *M. edulis* and *Jassa* spp. as well. The barnacles and algae may have created the right conditions for the settlement of juvenile blue mussels (Conell & Slatyer 1977), as i.e. *M. edulis* larvae prefer filamentous and thread like structures (Kerckhof et al 2009). This settlement pattern evolved into a dense, multilayered fouling community, comprising 100 % coverage of all panel surfaces by August 2021 and in 2022 already in May, without any decrease in coverage during the course of each year. Among the slightly higher mean temperatures in spring 2022 compared to 2021 it also has to be mentioned, that in 2022 test bodies were deployed earlier (March) than in the previous year (May). This allowed the collection of the spat fall from the very beginning of the spring season which probably resulted in higher abundances of barnacles in 2022. Barnacles are known key pioneer species, that colonize submerged structures in the initial phase of biofouling (Want et al 2021). Barnacles are known to reproduce early in the year from February on (Fish & Fish 2011; Kerckhof et al 2009) and are expected to dominate fouling communities in spring to early summer months (Southward 2008).

Due to the spatial dominance of the barnacles in the spring months of 2022, the absence of other key pioneer organisms e.g. hydroids (only sporadic occurrences in both years) may be explained on the test bodies in this work. However, exposed study sites like Nordergründe with harsh environmental conditions, such as high wave and (tidal-) current-induced forces, may have an important selective impact on fouling communities on artificial hard substrata (Denny 1987). High (tidal-) current flow may promote recruitment and growth of specific taxa through enhanced larval and nutrient transport (e.g. Bourget & Crisp 1975; Gaylord & Gaines 2000), whereas on the other hand it creates sufficient drag forces, inhibiting the settlement of certain organisms on the surface. This implies the settlement of taxa (e.g. blue mussel) which benefit from those

environment conditions. Increasing current velocities may result in the absence of soft foulants, except in niche spaces (acting as shelter), due to direct hydrodynamic stress (Coutts et al 2010). This was visible on the test bodies at the Nordergründe site with faster current speeds (0.59 ± 0.3-0.51 ± 0.25 m/s) where barnacles priorly dominated the fouling community, followed by *M. edulis* (both considered hard foulants) and *Jassa* spp. (soft foulants) in between the byssus threads of the blue mussel. In a study done by Beermann (2013) the creation of a mat-like surface made of amphipoda tubes was visible, and it is suggested that this prevents new larval settlement of other taxa (e.g. *M. edulis*) and smothers the underlying fouling taxa e.g. barnacles (De Mesel et al 2015). Similar observations were made in the present work (2021) as well, as the byssus threads and the in-niche living *Jassa* spp. and their tubes covered the prior settled barnacles. Consequently, in 2021 from September onwards mostly dead barnacles were studied under the above-mentioned mats at Nordergründe. This was not noticeable in the trials of 2022, where most barnacles were still alive, probably due a shorter period of sampling in that year. Additionally, as the size of the blue mussels expanded, the number of amphipods and their tubes decreased in both years. *Jassa* species have been recorded in high abundances on artificial structures such as buoys, windmill foundations or ship wrecks (e.g. Havermans et al 2007; Leonhard & Pedersen 2005). Amphipod species in the North Sea, such as *Jassa falcata* (Montagu 1808) demonstrate two reproduction maxima throughout the year; stronger in late spring to early summer and weaker in the winter months (Nair & Anger 1980). As hemi-sessile filter feeders, *Jassa* spp. build tubes, where each individuum feeds by extending their antennae into the water column (Dixon & Moore 1997). Newly submerged hard substrata can rapidly become covered by amphipoda tubes, mostly by recruitment and settlement of distributed juveniles from the surrounding waters (Havermans et al 2007). Beermann (2013) observed an all-year-around recruitment, which appeared almost insignificant during the winter months.

The reproductive maximum of blue mussels in German coastal seas occurs in the spring months, with a potential second spatfall in summer (Fish & Fish 2011). The free-swimming veliger larvae remain in the planktonic stage for up to four weeks before attaching on suitable substratum, then metamorphosing and settling by attaching their byssus filaments to the substrate. In both years only one pronounced reproduction cycle of the blue mussel and *Jassa* spp. were noticed on the test bodies. Though, no sampling of larval stages from the water body were conducted for any conclusion about intensities of spatfalls over the year. Additionally, it is known that the settlement of juvenile mussels and other larvae may be prevented by the filter feeding of the adult mussels (McQuaid

et al 2014). Earlier studies on *M. edulis* at Nordergründe displayed high larval densities in May with a decrease until September, whereby the highest growth in already settled mussels was observed in July (Buck 2007). This agrees with observations made on the test bodies in Nordergründe in this work.

Want et al (2021) stated that hard foulants (e.g. barnacles, bryozoa, blue mussels) in general benefit from less competition for space resources in higher flow velocity conditions and flourish more often in comparison to soft foulant organisms (e.g. hydrozoans). In 2022 the specific location of each panel (exposed to the current or sheltered behind the buoy body) were considered in the evaluation of the biofouling. The phenomena observed by Want et al (2021) at the Shetland Islands (UK), where some hard foulants (e.g. barnacles and mussels) dominated under rather exposed conditions (on steel panels) compared to soft foulants, was noticeable at Nordergründe as well. Considering the biology of the blue mussel, increased attachment and growth on the exposed side, compared to the sheltered panels, may partly be explained by their need of adequate transport of nutrients (phytoplankton) as filter feeders. High tidal current speeds at Nordergründe support appropriate nutrient content (Buck 2007). Additionally, the byssus filaments of blue mussels provide a tremendous competitive advantage compared to other organisms, thus enabling *M. edulis* to withstand the physical stresses of currents and waves more effectively (Brenner & Buck 2010).

Helgoland eulittoral

The eulittoral habitat of the Helgoland study site exhibited the lowest coverage in fouling communities of all habitats. In both years bare areas of stainless-steel were recorded until the early summer months, whereas the sessile biofouling composition was mostly comprised by Diatoms, green algae (*Ulva* spp. Linnaeus 1753), few brown algae as well as juvenile barnacles. Organisms living under constantly changing environmental conditions such as in the tidal zone with highly varying temperature, salinity, UV radiation and aridity must have adapted to these harsh conditions to survive in this habitat. *System B* (*MareLift*) is positioned at the inner quay wall of the north-east harbor, whereby the stainless-steel panels are orientated south-westerly. This resulted in extreme high temperatures during the summer months. The HOBO data logger attached to the mainboard detected a maximum temperature during low tide in August of both years of about 40.19 °C in 2021 and 48.39 °C in 2022. The settled *Ulva* spp. survived this heat probably due to forming a multi-layered mat to protect itself of abiotic stresses. The photoprotection and prevention of the loss of moisture was already observed in *Ulva* spp. under exposed upper intertidal conditions studied in southern Spain (Bischof et al 2002).

Only few barnacles survived on the eulittoral panels due to the extreme temperatures in the summer months. Noticeable was the colonization of Chirinomidae larvae exclusively on the eulittoral panels at Helgoland (limited contemplation on test bodies. The larvae require dense filamentous algae (e.g. *Ulva* spp.) or sand to build tubes (Krüger & Neumann 1983). Adults of Chirinomidae were sighted in the circumference of the *MareLift* eulittoral mainboards as well as in the splash zone at the Nordergründe site (*System A*). In Belgian wind farms larvae of the midge *Telmatogeton japonicus* (Tokunaga 1933) dominated the splash and high intertidal zone of the windmills (De Mesel et al 2015). Species of the Chirinomidae were also found at Helgoland (inside of the southern harbor) on sheltered PVC panels (Beermann 2013). Occurrences of this invasive species (originally from Japan) in eulittoral habitats were also observed in similar studies in wind farms in the southern North Sea e.g. Denmark (Leonhard & Petersen 2006). *Telmatogeton japonicus* larvae were firstly mentioned 1982 at Helgoland in studies done by Kronberg (1988), where scrape samples of rock surfaces (littoral fringe) were investigated in their species-composition. Therefore, it can be assumed that the observed larvae are the juveniles of *T. japonicus*.

Helgoland sublittoral

The fouling communities in the sublittoral habitat of Helgoland exhibited a very similar phenology as well as seasonal colonization pattern within both years. The initial settlement phase was dominated by brown algae in the spring months, initiating expected prior colonizer. After a decrease in panel coverage in early/mid-summer, whereby almost all algae vanished from the panels, the calcareous tube building polychaeta *Janua heterostropha* and various species of the class Ascidiacea dominated the fouling communities from mid/late summer onwards. Abundance and coverage increased throughout the course of the year, occupying free space and inhibiting settlement of other species (e.g. algae). Additionally, tube building amphipods were present from mid-summer on throughout the year, coincidently appearing at the same time as at the Nordergründe site (July 2021, June 2022) on all panels in both years. The here recorded Ascidians consisted mostly of colony-forming and social species and few solitary species. Beermann (2013) deployed PVC panels at a sheltered (southern harbor) and two exposed locations (northernly, moored at 1 m and 10 m depth) at the Helgoland study site. He observed that the solitary ascidian species *Ciona intestinalis* (Linnaeus 1767) and *Ascidiella aspersa* (Müller 1767) covered up 90 % of the sheltered panels after five months of exposure time. In contrast, at both exposed stations (5 months exposure) *Jassa* spp. and their turfs of tubes clearly dominated the biofouling community

(80-100 %), while other sessile species (e.g. barnacles, bivalves, bryozoans) were only present sporadically (Beermann 2013). This agrees with observations on deployed steel-panels at a sheltered site at the Shetland Islands which were dominated by large solitary Ascidiacea as well (Want et al 2021). In contrast, in the present study mostly encrusting colonies of the genus *Didemnum* spp. (Savigny 1816) and *Botryllus* spp. (Gaertner 1774) were recorded, whereas solitary species occurred only sporadically. In earlier sampling trials of the *EnviSim4Mare* project in 2020, test bodies made of black-steel were used exhibiting abundant occurrences of large solitary ascidians similar to the observations made by Beermann (2013) and Want et al (2015). With the deployment of *System B* (*MareLift*) in 2021 the black-steel was replaced with stainless-steel and corresponded with the absence of large solitary ascidia in the north-east harbor at Helgoland. Therefore, it can be assumed that these solitary ascidia species may not be able to settle on stainless-steel or prefer rougher substratum, respectively. To investigate further in this hypothesis, aluminum panels will be submerged along with stainless-steel panels at the *MareLift* in the early spring of 2023. Additionally, noticeable was the absence of *M. edulis* on all panels at Helgoland in both years (only sporadic occurrences of juveniles on sublittoral panels) in the north-east harbor. This observation was in strong contrast to the abundant occurrence of blue mussels underneath floating aluminum pontons in the same marina. Since stainless-steel was also in use at the Nordergründe site, where the blue mussel flourished, the absence on Helgoland panels cannot be explained by the used substrate material. It can rather be speculated that the orientation of the panels may be less suitable for the blue mussel. Owing to the predominant low current speeds in the marina, the vertical position of *System B* (including the test bodies) at the quay wall was probably adverse for the blue mussel for settling on the panels. Therefore, its competitiveness compared to other fouling taxa was reduced. In contrast the settlement and growth in the downward oriented position underneath the pontons could advantage the blue mussel over other taxa probably due to a modified current regime on a micro scale. To investigate further in the site-selection of *M. edulis* the mentioned aluminum panels will be fixed and analyzed in 2023 to assess the importance of the substrate material and position.

Similar to the present study panels exposed at a sheltered Shetland Island site exhibited the dominance of the encrusting calcareous tube worm *Spirobranchus triqueter* (Linnaeus 1758) during the initial fouling phase (Want et al 2021). This species is confamiliar with *J. heterostropha* (Serpulidae), here detected on the panels of the sublittoral in Helgoland. Consequently, this suggests that *J. heterostropha* may prefer sheltered sites for settling. Though, the worms were also found at an exposed site in a

more recent study on the coastline of Ceredigion (Wales) suggesting that the species could likely be a generalist in terms of wave height and current conditions (Wilson & Hayek 2020). Even though, the calcareous tube worm appeared in high abundances, it did not show a strong competition for space, as they were overgrown by *Didemnum* spp. colonies from mid-summer (Jul/Aug) onwards. Juveniles of *Didemnum* spp. were found from July through November, peaking from late August through early September on the west Atlantic coast of the USA (Connecticut; Bullard et al 2007). Peak cover and highest abundances in the Helgoland sublittoral also occurred during summer to early fall. *Didemnum* spp. are common in sublittoral areas nearshore and offshore (Bullard et al 2007) and by overgrowing other fouling taxa, which demonstrate a strong competitive ability, which was also observed in the present study.

5 Conclusions and Outlook

Both developed systems provide a basis for sampling and monitoring of living fouling species in exposed and sheltered locations under different environmental conditions. The biofouling collectors may be an important tool for adequate risk appraisal (e.g. load and load-flows) in the marine renewable energy sector when developing new offshore structures. Overall, *System A* and *B* offer a solid opportunity for future biofouling research as well as potentially different research approaches in exposed and sheltered areas. An additional biofouling collector on the basis of the *Pentagon* (*System A*) is already planned to be deployed at a third study site in Wilhelmshaven (Germany) within the *EnviSim4Mare* project.

Fouling communities studied in this work showed a great distinction in spatial and seasonal composition and exhibited the profound influence of environmental factors on the development of biofouling. In regard to the course of time, Nordergründe site fouling communities will likely develop into a *Mytilus edulis*-*Jassa* spp. dominated stage, the Helgoland eulittoral habitat will similarly remain of the observed community of *Ulva* spp. and Chirinomidae larvae due to the extreme variations in environmental parameters (e.g. temperature, salinity). Sublittoral communities of Helgoland will likely decrease in species-richness and develop into an ascidian-dominated composition due to their strong dominance and competitiveness in overgrowing other organisms.

6 References

Abarzua S & Jakubowski S (1995) Biotechnological investigation for the prevention of biofouling Biological and biochemical principles for prevention of biofouling. Marine ecol. Prog. Ser. Vol 123, pp 301-312.

Almeida LP & Coolen J (2020) Modelling thickness variations of macrofouling communities on offshore platforms in the Dutch North Sea. Journal Sea. Res. Vol 156, 101836 I Elsevier Enhanced Reader https://doi.org/10.1016/j.seares.2019.101836

Al-Yacouby A Kurian V Sebastian A Liew M & Idichandry V (2014) Effect on marine growth on hydrodynamic coefficients of rigid tubular cylinders. Appl. Mech. Mater. Vol 567 pp 247-252.

Becker GA Dick S & Dippner JW (1992) Hydrography of the German Bight. Hamburg, Germany: Mar. Ecol. Prog. Ser. Vol 91 pp 9-18.

Beermann J (2013) Ecological differentiation among Amphipod species in marine fouling communities: Studies on sympatric species of the genus *Jassa* Leach, 1814 (Crustacea, Amphipoda). Berlin: Dissertation p 98

Beermann J & Franke HD (2011) A supplement to the amphipod (Crustacea) species inventory of Helgoland (German Bight, North Sea): indication of rapid recent change. Marine Biological Association of the United Kingdom: Marine Biodiversity Records Vol 4 pp 1-15 https://doi.org/10.1017/S1755267211000388

Bell R Gray S & Jones O (2017) North Atlantic storm driving of extreme wave heights in the North Sea. J. Geophys. Res. Oceans Vol 122 pp 3253-3268.

Bischof K Peralta G Kräbs G Van den Poll WH Perez-Llorens JL & Breeman A (2002) Effects of solar UV-B radiation on canopy structure of *Ulva* communities from southern Spain. J. Exp. Bot. Vol 379 pp 2411–2421 https://doi.org/10.1093/jxb/erf091

Böttcher J (2013) Handbuch Offshore-Windenergie. Oldenbourg Wissenschaftsverlag p 89 https://doi.org/10.1524/9783486717761

Bourget E & Crisp D (1975) Factors affecting deposition of the shell in *Balanus balanoides* (L.). J Mar Biol Ass Vol 55 pp 231-249 https://doi.org/10.1017/S0025315400015873

Brenner M & Buck BH (2010) Attachment properties of blue mussel (*Mytilus edulis* L.) byssus threads on culture-based artificial collector substrates. Aquacultural Engineering, Vol 42(3), pp 128–139. https://doi.org/10.1016/j.aquaeng.2010.02.001

Brüning TL (2021) An operational, assimilative model system for hydrodynamic and biogeochemical applications for German coastal waters pp 6–15 https://doi.org/10.23784/HN118-01

BSH (2019) Mündungen der Alten Weser und der Neuen Weser, Innerer Teil. Kartennr. 1240 Ausgabe 3 Vlll

BSH (2022) Nutzungskarten. Accessed August 24, 2022 https://www.bsh.de/DE/THEMEN/Offshore/Nutzungskarten/nutzungskarten_node.html

Buck BH (2007) Experimental trials on the feasibility of offshore seed production of the mussel *Mytilus edulis* in the German Bight: installation, technical requirements and environmental conditions. Helgol. Mar. Res. Vol 61, pp 87-101

Buck BH & Buchholz CM (2004) The offshore-ring: A new system design for the open aquaculture of macroalgae. J. Appl. Phycol. Vol 16 pp 355-368.

Bullard S Lambert G Carman MR Whitlatch R Ruiz G . . . Heinonen K (2007) The colonial ascidian *Didemnum* sp. A: Current distribution, basic biology and potential threat to marine communities of the northeast and west coasts of North America. Journal of Experimental Marine Biology and Ecology, Proceedings of the 1st International Invasive Sea Squirt Conference Vol 342 pp 99–108 https://doi.org/10.1016/j.jembe.2006.10.020

Bundesministerium für Umwelt und Naturschutz (BMU) (2018) Zustand der deutschen Nordseegewässer, Aktualisierung der Anfangsbewertung nach § 45c, der Beschreibung des guten Zustands der Meeresgewässer nach § 45d und der Festlegung von Zielen nach § 45e des Wasserhaushaltsgesetz zur Umsetzung der Meeresstrategie-Richtlinien. Bonn: BMU pp 18-22.

Cao S Wang J Chen H & Chen D (2011) Progress of marine biofouling and antifouling technologies. Chin. Sci. Bull. Vol 56 pp 598-612.

Caspers H (1952) Der tierische Bewuchs an Helgoländer Tonnen. Helgoland: Wiss. Meer. Vol 4 pp 138-160

Clearman B (1988) Transportation-markings database: International marine aids to navigation Series: Transportation Markings: A Study in Communication. Oregon, USA: Vol 1, parts C and D. 2nd edition, p 230

Colwell R (1983) Biotechnology in the marine sciences New Series Vol 222 No 4619 pp. 19-24

Connell J & Slatyer R (1977) Mechanisms of succession in natural communities and their role in community stability and organization. The American Naturalist Vol 11 pp 1119-1144

Coutts A Richard DFP Hewitt C & Connell S (2010) Effect of vessel voyage speed on survival of biofouling organisms: implications for translocation of non-indigenous marine species. Biofouling Vol 26 pp 1-13. https://doi.org/10.1080/08927010903174599

Dannheim J (2015) Den Meeresboden im Blick: das Leben in Zeiten der Offshore-Windenergie. Nordenham: BUND Wesermarsch, Moorseer Mühle, Nordenham

Dayton P (1971) Competition, disturbance, and community organization: The provision and subsequent utilization of space in a rocky intertidal community. Ecol. Monogr., Vol 41 pp 351–389

De Kluijver MJ (1991) Sublittoral hard substrate communities off Helgoland. Meeresunters. Vol 45 pp 317-344 https://doi.org/10.1007/BF02365523

De Mesel I Kerckhof F Norro A Rumes B & Degraer S (2015) Succession and seasonal dynamics of the epifauna community on offshore wind farm foundations and their role as stepping stones for non-indigenous species. Hydrobiologia Vol 756 pp 37–50

Denny M (1987) Life in the maelstrom: the biomechanics of wave-swept rocky shores. Trends Ecol Evol. Vol 2 pp 61–66 https://doi.org/10.1016/0169-5347(87)90150-9

Deutscher Wetterdienst (2022) Wetter- und Klimalexikon. Accessed October, 17 2022 https://www.dwd.de/DE/service/lexikon/Functions/glossar.html?lv3=100390&lv2=100310

Deutsche WindGuard (2022) Windenergie-Statistik 1. Halbjahr 2022. Accessed November 19, 2022 https://www.windguard.de/id-1-halbjahr-2022.html

Dixon I & Moore P (1997) A comparative study on the tubes and feeding behaviour of eight species of corophiid Amphipoda and their bearing on phylogenetic relationships within the Corophioidea. Philosophical Transactions of the Royal Society of London B: Biological Sciences Vol 352 pp 93-112

Dörjes J Gadow D Reineck HE & Singh IB (1970) Sedimentologie und Makrozoobenthos der Nordergründe und Außenjade (Nordsee). Senckenb. Marit. Vol 2 pp 31-59

Figge K (1981) Karte zur Sedimentverteilung in der Deutschen Bucht im Maßstab 1: 250000. Deutsches Hydrographisches Institut Nr. 2900.

Fish & Fish (2011) A student's guide to the seashore (Bd. 3). New York: Cambridge University Press pp 4-5

Gaylord B & Gaines S (2000) Temperature or transport? Range limits in marine species mediated solely by flow. Am Nat Vol 155 pp 769-789 https://doi.org/10.1086/303357

Goseberg PD (2019) Wie Muscheln, Algen und Co. Bauwerke im Meer belasten. Accessed August 22, 2022 https://magazin.tu-braunschweig.de/pi-post/wie-muscheln-algen-und-co-bauwerke-im-meer-belasten/

Hannemann O (2022) OpenSeaMap - die freie Seekarte. Stubben. Accessed October 27, 2022 https://www.openseamap.org/index.php?id=openseamap&no_cache=1

Havermans C De Boyer C Mallefet J & Zintzen V (2007) Dispersal mechanisms in amphipods: a case study of *Jassa herdmani* (Crustacea, Amphipoda) in the North Sea. Marine Biology Vol 153 pp 83–89

Hellio C & Yebra D (2009) Advances in Marine Antifouling Coatings and Technologies. Boca Ranton, FL, USA, CRC Press p 785

Hopkins G Davidson I Georgiades E Floerl O Morrisey D & Cahill P (2021) Managing biofouling on submerged static artificial structures in the marine environment - assessment of current and emerging approaches. Front. Mar. Sci. Vol 8 759194.

Horn H (1974) The Ecology of Secondary Succession Annual. Review of Ecology and Systematics Vol 5 pp 25-37

Huthnance J (1991) Physical oceanography of the North Sea. Ocean and Shoreline Management Vol 16 pp 199-231 https://doi. org/10.1016/0951-8312(91)90005-M

Isbert W Lindemann C Lemburg J Littmann M Tegetoff K Goseberg N . . . Buck BH (2022 [in review]) A conceptual basis for surveying fouling communities at exposed and sheltered sites at sea: feasible designs with exchangeable test bodies for in-situ biofouling collection. Bremerhaven: Alfred-Wegener-Institut für Polar- und Meeresforschung (AWI).

IWR (2022) Studie: Kompromisse bei gemeinsamer Flächennutzung ermöglichen ambitionierten Offshore-Ausbau. Berlin. Accessed August 24, 2022 https://www.offshore-windindustrie.de/news/nachrichten/artikel-38042-studie-kompromisse-bei-gemeinsamer-flaechennutzung-ermoeglichen-ambitionierten-offshore-ausbau

Jahn C (2020) Charakteristika von Standorten für On- und Offshore-Windparks. Hamburg: Technische Universität Hamburg, Institut für Maritime Logistik. Accessed October 19, 2022 https://www.forschungsinformationssystem.de/servlet/is/405524/

Jänicke L Ebener A Dangendorf S Arns A Schindelegger M Niehüser S . . . Jensen J (2021) Assessment of Tital Range Changes in the North Sea from 1958 to 2014. Journal of Geophysical Research: Oceans, Vol 126 (1) pp 1-18, Article e2020JC016456. https://doi.org/10.1029/2020jc016456

Johnson L & Strathmann R (1989) Settling barnacle larvae avoid substrata previously occupied by a mobile predator. J. Exp. Mar. Biol. Ecol. Vol 128 pp 87–103

Jusoh I & Wolfram J (1996) Effects of marine growth and hydrodynamic loading on offshore structures. Jurnal Mekanikal, Vol 1 (1) pp 77-96 ISSN 0127-3396

Kerckhof F Rumes B & Degraer S (2019) About *Mytilisation* and *Slimefication*: A decade of the fouling assemblages on wind mills off the Belgian Coast. In Degraer R Brabant B Rumes & L Vigin, Environmental impacts of offshore wind farms in the Belgian Part of the North Sea - Marking a decade of monitoring, reserach and innovation (pp 73-84). Brussels: Royal Belgian Institute of Natural Sciences, OD Natural Environment, Marine Ecology and Management.

Kerckhof F Norro A Jaques T & Degraer S (2009) Early colonisation of a concrete offshore windmill foundation by marine biofouling on the Thornton Bank (southern North Sea) Management Unit of the North Sea Mathematical Models (MUMM), Gulledelle 100, Brussels, Belgium pp 40-51.

KernD (2022) Zahlen, Kernkraftwerke in Betrieb. Accessed November 11, 2022 https://www.kernd.de/kernd/themen/strom/Zahlen-und-Fakten/01_index.php#anchor_f93853ce_Accordion-Kernkraftwerke-in-Betrieb

Klijnstra J Zhang X van der Putten S & Röckmann C (2017) Chapter 5 - Technical Risks of Offshore Structures in: Aquaculture Perspective of Multi-Use Sites in the Open Ocean: The Untapped Potential for Marine Resources in the Anthropocene (Buck BH et al). Springer Link https://doi:10.1007/978-3-319-51159-7_5, pp 115-127

Korevaar C (1990) North Sea climate based on observations from ships and lightvessels. Kluwer Academic Publishers, ISBN 0-7923-0664-3. 10.1002/joc.3370110814

Kronberg I (1988) Structure and adaptation of the fauna in the black zone (littoral fringe) along rocky shores in northern Europe. Kiel, Germany: Mar. Ecol. Prog. Ser. Vol 49 pp 95-108

Krone R Gutow LJ & Schröder A (2013) Epifauna dynamics at an offshore foundation - implications of future wind power farming in the North Sea. Mar. Environ. Res. Vol 85 pp 1-12

Krüger M & Neumann D (1983) Die Temperaturabhängigkeit semilunarer und diurnaler Schlüpfrhythmen bei der intertidalen Mücke *Clunio marinus* (Diptera, Chironomidae). Helgoländer Meeresunters. Vol 36 pp 427-464

Langhamer O Wilhelmsson D & Engström J (2009) Artificial reef effect and fouling impacts on offshore wave power foundations and buoys - a pilot study. Estuar Coast Shelf, Vol 82 pp 426-432 https://doi:10.1016/j.ecss.2009.02.009

Lehaitre M Delauney L & Compère C Babin M Roesler CS Cullen JJ (2008) Biofouling and underwater measurements in Real-Time Observation. Paris, France., Eds.; UNESCO Publishing, pp 463-493

Leonhard S & Pedersen J (2006) Benthic communities at Horns Rev before, during and after construction of Horns Rev Offshore Wind Farm. Final report 2005. Udarbejdet af Bio/consult as for ELSAM Engineering Vol 96

Lincoln R Boxshall G & Clark P (1998) A dictionary of ecology, evolution and systematics Cambridge University Press, UK pp 361

Loxton J Macleod AK Collin T Machado I . . . Miller R (2017) Setting an agenda for biofouling research for the marine renewable energy industry. International Journal of Marine Energy Vol 19 pp 292-303

Luther G (1964) "Helgoland"- an underwater laboratory for rough sea conditions. Helgoländer Wiss. Meeresunters. Vol 24 pp 45-53 https://doi.org/10.1007/BF01609498

MCQuaid CD, Porri F, Nicastro KR, Zardi GI (2014) Simple, scale-dependent patterns emerge from very complex effects - an example from the intertidal mussels *Mytilus galloprovincialis* and Perna perna. Oceanography and Marine Biology: An Annual Review Vol 53 pp 127-156

Menchaca I Zorita I Rodríguez-Ezpeleta N Erauskin C Erauskin E Liria P . . . Urtizberea I (2014) Guide for the evaluation of biofouling formation in the marine environment Revista de Investigacion Marina Vol 21(4) pp 89-99

Momber AW Plagemann P & Stenzel V (2015) Performance and integrity of protective coating systems for offshore wind power structures after three years under offshore site conditions. Renew. Energy Vol 74 pp 606-617

Morison J O'Brien M Johnson J & Schaaf S (1950) The forces exerted by surface waves on piles Petroleum Transactions Vol 189 (TP 2846) p 149

Nair K & Anger K (1980) Seasonal variation in population structure and biochemical composition of *Jassa falcata* (Crustacea, Amphipoda) off the Island of Helgoland (North Sea). Estuarine and Coastal Marine Science Vol 11 pp 505-513

Orejas C Joschko T Schröder A Dierschke J Exo M Friedrich E Hill R Hüppop O Pollehne F Zettler ML Bochert R (2005) Ökologische Begleitforschung zur Windenergienutzung im Offshore-Bereich auf Forschungsplattformen in der Nord- und Ostsee (BeoFINO) pp 356 Bremerhaven, Germany: Alfred- Wegener-Institute (AWI) Bremerhaven.

Pomerat C & Weiss C (1946) The influence of texture and composition of surface on the attachment of sedentary marine organisms. Biol. Bull. Vol 91 pp 57-65

Putzar B & Malcherek A (2015) Entwicklung und Anwendung eines Langfrist-Morphodynamikmodells für die deutsche Bucht. Die Küste Vol 83 pp 117-145

Quante M & Colijn F (2016) North Sea region change assessment. New York, NY: Springer Nature https://doi. org/10.1007/978-3-319-39745-0 ISBN: 978-3-319-39743-6

Raffaelli D & Hawkins S (1999) Intertidal Ecology. Dordrecht, Netherlands: Kluwer Academic Publishers, p 365

Railkin A (2003) Marine Biofouling: Colonization Processes and Defences. Boca Raton, FL, USA: CRC Press: p 303

Richmond M & Seed R (1991) A review of marine macrofouling communities with special reference to animal fouling. Biofouling, Vol 3 pp 151-186

Schröder A Gutow L Jaschko T Krone R Gusky & M Paster (2008) Benthos ökologische Auswirkungen von Offshore-Windparks in der Nordsee BeoFINO ll pp 123-130. Prozesse im Nahbereich der Piles. Alfred-Wegener-Institute Bremerhaven, Bremerhaven, Germany.

Southward A (2008) Barnacles: keys and notes for the identification of British species. Field Studies Council Vol 57

Stiftung Offshore Windenergie (2021) Sauberer Strom vom Meer. Accessed August 22, 2022 https://www.offshore-stiftung.de/offshore-windenergie

Sündermann J & Pohlmann T (2011) A brief analysis of the North Sea physics. Oceanologia, Vol 53 pp 663-689

Tanaka N & Asakawa A (1988) Allelopathic effect of mucilage released from brown alga *Sargassum horneri* on marine diatoms. Nippon Susian Gakk Vol 54 pp 1711-1714

Titah-Benbouzid H & Benbouzid M (2017) Biofouling issue on marine renewable energy converters: A state of the art review on impacts and prevention. Int. J. Energy Convers, Vol 5 pp 67-78

Van Der Stap T Coolen J & Lindeboom H (2016) Marine Fouling Assemblages on Offshore Gas Platforms in the southern North Sea: Effects of Depth and Distance from Shore on Biodiversity. PLoS ONE, 11, e0146324.

Vinagre PA Simas T Cruz E Pinori E & Svenson J (2020) Marine Biofouling: A European Database for the Marine Renewable Energy Stor. Journal of Marine Science and Engineering Vol 8 pp 1-27

Wahl M (1989) Marine epibiotic I. Fouling and antifouling: Some basic aspects. Mar. Ecol. Prog. Ser. Vol 58 pp 175-189

Want A & Porter J (2018) BioFREE: An international Study of Biofouling impacts on the marine renewable energy industry. Kobe, Japan: Institute of Electrical and Electronics Engineers (IEEE): Oceans-MTS/IEEE Kobe Techno-Oceans (OTO) pp 1-7

Want A Bell M Harris R Hull M Long C & Porter J (2021) Sea-trial verification of a novel system for monitoring biofouling and testing anti-fouling coatings in highly energetic environments targeted by the marine renewable energy industry. Biofouling. pp 1-19 https://doi:10.1080/08927014.2021.1928091

Want A Crawford R Kakkonen J Kiddie G Miller S Harris RE & Porter J (2017) Biodiversity characterisation and hydrodynamic consequences of marine fouling communities on marine renewable energy infrastructure in the Orkney Islands Archipelago. Scotland, UK: Biofouling Vol 33 pp 567-579

Weisse R & Günther H (2007) Wave climate and long-term changes for the Southern North Sea obtained from a high-resolution hindcast 1958-2002. Ocean Dyn. Vol 57 pp 161-172. https://doi:10.1007/s10236-006-0094-x

Wilson B & Hayek LA (2020) Calcareous meiofauna associated with the calcareous alga *Corallina officinalis* on bedrock and boulder-field shores of Ceredigion, Wales, UK. Journal of the Marine Biological Association of the United Kingdom Vol 100 pp 1205–1217 https://doi.org/10.1017/S0025315420001174

Wiltshire K Boersma M Carstens K Kraberg A Peters S & Scharfe M (2015) Control of phytoplankton in a shelf sea: Determination of the main drivers based on the Helgoland Roads Time Series. Journal of Sea Research Vol 105. https://doi.org/10.1016/j.seares.2015.06.022

WSA (2021) Data for water temperature and salinity at monitoring station lighthouse „Alte Weser“, Wasserstraßen- und Schifffahrtsverwaltung des Bundes, Zentrales Datenmanagement (ZDM) Küstendaten. WSA. Accessed October 26, 2022 www.küstendaten.de

Yebra D Kiil S & Dam-Johansen K (2004) Antifouling technology- Past, present and future steps towards efficient and environmentally friendly antifouling coatings. Prog. Org. Coat. Vol 50 pp 75–104

Zeiler M Milbrandt P Plüss A & Valerius J (2018) Modellierung großräumiger Sedimenttransporte in der Deutschen Bucht (Nordsee). Die Küste Vol 86 pp 399-423

Zhang H Cao W Wu Z Song X Wang J & Yan T (2015) Biofouling on deep-sea submersible buoy systems off Xisha and Dongsha Islands in the northern South China Sea. Int. Biodeterior. Biodegradation Vol 104 pp 92-96

7 Annex

7.1 Environmental conditions at both sides

Table 3 Current velocity average [m/s] in 1 m depth ± SD (Brüning 2021)

	Current velocity average [m/s]					
	Helgoland (northward directed current)	**Nordergründe (eastward directed current)**	**Nordergründe (northward directed current)**	**± SD Hel north**	**± SD Nor east**	**± SD Nor north**
2021 Jan	0.49	0.60	0.53	0.29	0.30	0.25
Feb	0.49	0.62	0.52	0.29	0.30	0.25
Mar	0.49	0.63	0.55	0.29	0.31	0.26
Apr	0.49	0.63	0.56	0.29	0.32	0.27
May	0.49	0.62	0.55	0.29	0.31	0.27
Jun	0.49	0.65	0.56	0.29	0.31	0.27
Jul	0.49	0.64	0.56	0.29	0.30	0.25
Aug	0.49	0.62	0.54	0.29	0.30	0.25
Sep	0.49	0.62	0.54	0.29	0.30	0.25
Oct	0.49	0.59	0.53	0.29	0.31	0.26
Nov	0.49	0.60	0.54	0.29	0.31	0.26
Dec	0.49	0.61	0.54	0.29	0.31	0.26
2022 Jan	0.49	0.51	0.44	0.29	0.19	0.25
Feb	0.49	0.50	0.43	0.29	0.19	0.24
Mar	0.49	0.57	0.45	0.29	0.20	0.27
Apr	0.49	0.55	0.45	0.29	0.20	0.27
May	0.49	0.54	0.44	0.29	0.20	0.26
Jun	0.49	0.54	0.44	0.29	0.20	0.25
Jul	0.49	0.54	0.45	0.29	0.20	0.25
Mean 2021	0.49	0.62	0.54	0.29	0.31	0.26
Mean 2022	0.49	0.54	0.44	0.29	0.20	0.26

Table 4 Water temperature average [°C] in 1 m depth ± SD (Brüning 2021)

	Temperature average [°C]			
	Nor	**Hel**	**± SD Nor**	**± SD Hel**
2021 Jan	3.48	5.63	0.88	0.7
Feb	1.40	3.33	1.72	0.58
Mar	4.86	4.10	0.8	0.63
Apr	7.19	6.02	1.05	0.83
May	10.52	8.61	1.56	1.06
Jun	17.10	13.60	1.76	1.86
Jul	19.49	16.58	0.67	1.11
Aug	18.09	17.74	0.64	0.31
Sep	17.32	17.34	0.82	0.46
Oct	13.10	14.50	1.54	1.23
Nov	9.40	11.26	1.23	1.08
Dec	4.95	7.95	1.33	0.82
2022 Jan	4.75	6.67	0.57	0.71
Feb	5.24	5.58	0.31	0.23
Mrz	5.61	6.43	0.96	0.56
Apr	8.05	7.82	1.66	1.13
Mai	12.56	11.19	1.5	1.02
Jun	16.42	14.63	1.7	1.12
Jul	18.28	17.1	0.65	0.58
Aug		19.07		0.66
Sep		17.26		1.02
Oct		15.25		0.43
Mean 2021	10.58	10.55	6.07	5.07
Mean 2022	10.13	11.73	5.20	4.61

Table 5 Salinity average [g/kg] in 1 m depth ± SD (Brüning 2021)

	Salinity average [g/kg]			
	Nor	**Hel**	**± SD Nor**	**± SD Hel**
2021 Jan	33.00	34.47	0.73	0.11
Feb	30.85	34.21	1.7	0.2
Mar	30.56	33.20	2.35	0.73
Apr	28.42	32.22	2.05	0.42
May	30.52	32.73	1.94	0.37
Jun	29.71	32.95	1.36	0.66
Jul	30.68	33.30	1.68	0.35
Aug	31.63	33.06	1.33	0.37
Sep	29.99	32.71	1.48	0.16
Oct	31.67	32.58	0.57	0.19
Nov	31.96	32.46	0.55	0.3
Dec	31.93	33.63	0.95	0.79
2022 Jan	33.29		0.6	
Feb	33.46		0.39	
Mrz	31.16		1.69	
Apr	31.56		1.8	
Mai	31.70		1.46	
Jun	32.00		0.85	
Jul	31.85		0.73	
Mean 2021	30.91	33.13	1.17	0.66
Mean 2022	32.15		0.82	

Table 6 Water temperature average [°C] of HOBO data logger ± SD

Temperature average HOBO [°C]

	HelEu	HelSub	± SD HelEu	± SD HelSub
2021 Aug	18.85		4.41	
Sep	18.54		4.17	
Oct	14.24		2.34	
Nov	10.54		2.36	
Dec	6.80	8.00	2.68	0.82
2022 Jan	6.42	6.67	1.70	0.71
Feb	6.03	5.58	2.53	0.23
Mrz	7.14	6.43	4.22	0.56
Apr	9.22	7.82	5.03	1.13
Mai	12.93	11.19	4.56	1.02
Jun	16.36	14.63	5.30	1.12
Jul	18.05	17.10	4.04	0.58
Aug	21.25	19.07	6.68	0.66
Sep	17.21	17.26	4.66	1.02
Oct	14.93	15.25	2.80	0.43
Mean	13.23	11.73	4.85	4.61

7.2 General development of sessile biofouling taxa on test bodies

Table 7 Fouling rates of single taxa [%] in 2021

2021 Fouling Rate of single taxa [%]

HelEu21		Free space	Diatoms	Brown algae	Green algae	Red algae	Sponges	Anthozoans	Hydrozoans	Moss animals	Tube buil. worms	Amphipoda tubes	Barnacle	Blue mussel	Tunicates
	May	99.2	0.8	0.0	0.0	0.0	0.0	0.0	0.0	0.0	0.0	0.0	0.0	0.0	0.0
	Jun	98.8	0.2	0.0	0.8	0.0	0.0	0.0	0.0	0.0	0.0	0.0	0.1	0.0	0.0
	Jul	67.9	0.0	0.0	20.1	0.0	0.0	0.0	0.0	0.0	0.0	0.3	11.5	0.0	0.2
	Aug	21.7	0.0	0.0	77.3	0.0	0.0	0.0	0.0	0.0	0.0	0.0	1.0	0.0	0.0
	Sep	4.3	0.0	0.0	94.3	0.0	0.0	0.0	0.0	0.0	0.0	0.0	1.3	0.0	0.0
	Nov	7.3	13.3	0.3	76.0	1.7	0.0	0.0	0.0	0.0	0.0	0.0	1.3	0.0	0.0
	Dec	21.7	0.0	0.0	77.3	0.0	0.0	0.0	0.0	0.0	0.0	0.0	1.0	0.0	0.0
HelSub21															
	May	23.3	0.4	75.8	0.0	0.0	0.0	0.0	0.0	0.0	0.3	0.0	0.1	0.1	0.0
	Jun	53.3	0.3	39.2	5.0	0.0	0.0	0.0	0.3	0.0	1.3	0.1	0.5	0.0	0.0
	Jul	64.7	0.0	4.5	3.7	0.1	0.2	0.5	1.7	0.8	16.8	2.2	2.4	0.4	2.0
	Aug	5.8	0.0	0.0	0.0	0.0	0.0	0.2	0.0	0.5	27.8	3.7	1.5	0.0	60.5
	Sep	6.2	0.0	0.3	0.5	0.3	0.0	0.3	0.3	0.7	38.0	4.0	1.3	0.0	48.0
	Nov	11.4	0.0	0.7	1.0	1.3	0.0	0.6	0.2	2.2	35.0	27.3	4.0	0.0	16.3
	Dec	28.6	0.0	0.3	0.0	2.0	0.3	0.5	0.0	0.2	19.8	12.0	4.7	0.0	31.7
NorSub21															
	Jun	36.7	0.0	7.7	3.7	0.0	0.0	0.0	20.0	1.3	0.0	0.1	29.7	0.9	0.0
	Jul	12.7	0.0	29.0	3.0	0.0	0.0	0.0	2.3	4.0	0.0	38.3	9.3	1.3	0.0
	Aug	0.9	0.0	0.2	0.2	0.0	0.0	1.0	0.0	0.0	0.0	17.7	0.0	80.0	0.0
	Sep	2.3	0.0	0.0	0.0	0.0	0.0	0.0	0.0	0.0	0.0	81.7	2.0	14.0	0.0
	Nov	2.3	0.0	0.0	0.0	0.0	0.0	0.0	0.0	0.0	0.0	2.7	0.0	95.0	0.0

Table 8 Fouling rates of single taxa [%] in 2022

2022 Fouling Rate of single taxa [%]

HelEu22		Diatoms	Brown algae	Green algae	Red algae	Sponges	Anthozoans	Hydrozoans	Moss animals	Tube buil. worms	Amphipoda tubes	Barnacle	Blue mussel	Tunicates	Free space
	Apr	0.1	0.1	0.2	0.0	0.0	0.0	0.0	0.0	0.0	0.0	0.0	0.0	0.0	99.7
	May	1.7	0.3	5.7	0.0	0.0	0.0	0.0	0.0	0.0	0.0	0.0	0.0	0.0	92.3
	Jun	6.7	36.7	26.3	0.0	0.0	0.0	0.0	0.0	0.0	2.0	4.3	0.0	0.0	24.0
	Jul	19.7	0.0	61.3	0.0	0.0	0.0	0.0	0.0	0.0	0.0	4.3	0.0	0.0	14.7
	Aug	31.0	1.0	64.3	0.0	0.0	0.0	0.0	0.0	0.0	0.0	1.0	0.0	0.0	2.7
	Sep	1.0	1.7	95.0	0.0	0.0	0.0	0.0	0.0	0.0	0.3	0.0	0.0	0.0	2.0
	Oct	1.7	1.7	70.0	0.0	0.0	0.0	0.0	0.0	0.0	0.0	0.0	0.0	0.0	26.7
HelSub22															
	Apr	1.0	59.7	0.7	0.0	0.0	0.0	0.0	0.0	0.0	0.0	0.0	0.0	0.0	38.7
	May	6.7	81.3	2.3	0.7	0.0	0.0	0.7	0.0	0.3	2.3	0.7	0.0	0.0	5.0
	Jun	0.0	2.0	3.7	0.3	0.0	0.0	1.7	0.3	10.3	4.7	5.7	0.2	0.0	71.2
	Jul	11.2	0.5	1.2	0.0	0.0	0.0	1.4	2.7	14.3	7.0	8.0	0.2	33.7	19.8
	Aug	0.0	2.7	1.5	3.3	0.0	0.0	1.2	2.5	33.3	3.3	7.0	0.2	24.3	20.7
	Sep	0.0	4.7	1.2	5.0	1.2	0.2	1.3	1.0	26.7	14.0	13.3	0.2	17.0	14.3
	Oct	0.0	12.3	1.7	6.7	2.7	0.0	2.2	2.4	15.3	11.3	12.3	0.0	25.3	7.7
NorSub22															
	April	0.0	79.0	1.5	0.0	0.0	0.0	0.0	0.0	0.0	0.0	1.0	0.0	0.0	18.5
	Mai	0.0	28.7	0.7	0.0	0.0	0.0	0.0	0.0	0.0	1.0	41.3	27.3	0.0	1.0
	Jun	0.0	0.0	0.0	0.0	0.0	0.0	0.0	0.3	0.0	16.3	13.3	70.0	0.0	0.0
	Jul	0.0	0.0	0.0	0.0	0.0	0.3	0.3	0.3	0.0	9.8	34.3	54.7	0.0	0.2

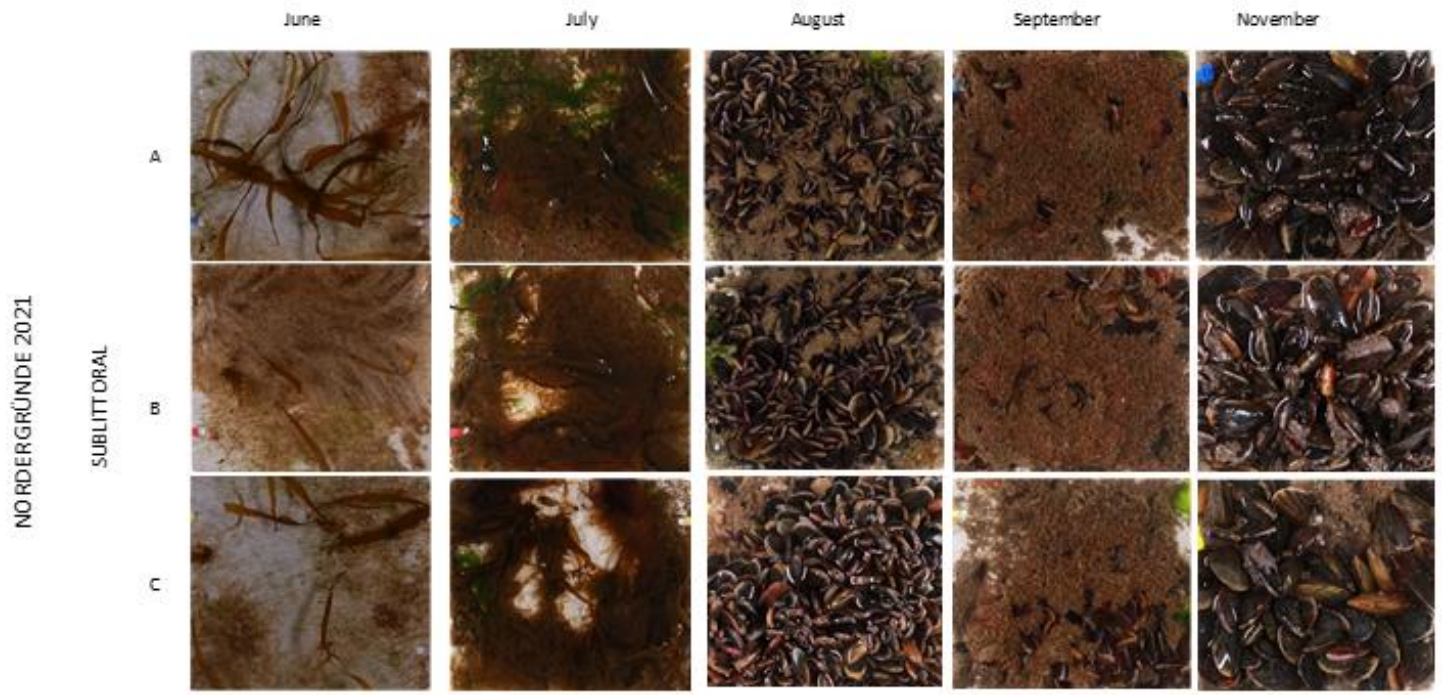

Figure 20 Monthly photographs of biofouling for Nordergründe in 2021 (Nor). Sampling was done from June to November (no sampling in October)

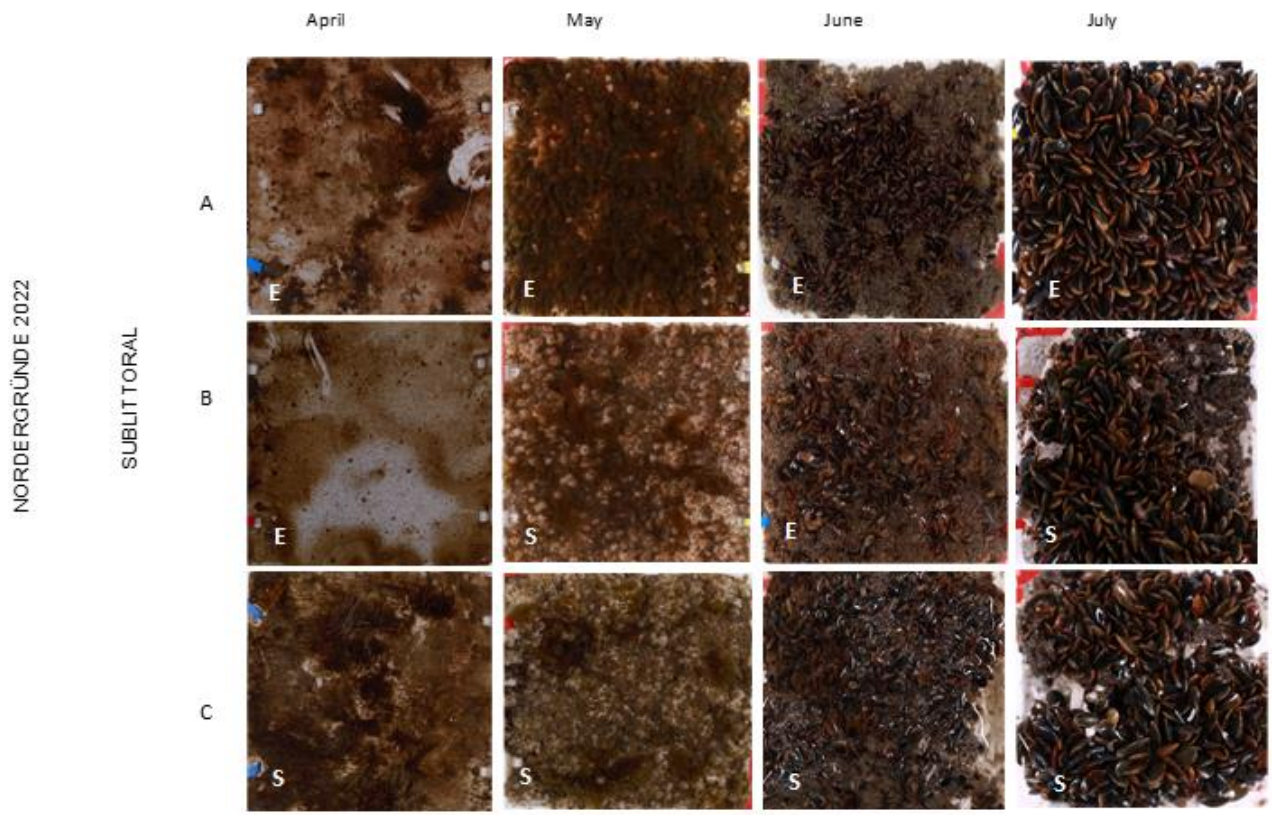

Figure 21 Monthly photographs of biofouling for Nordergründe in 2022 (Nor). Sampling was done from April to July. S=sheltered, E=exposed conditions

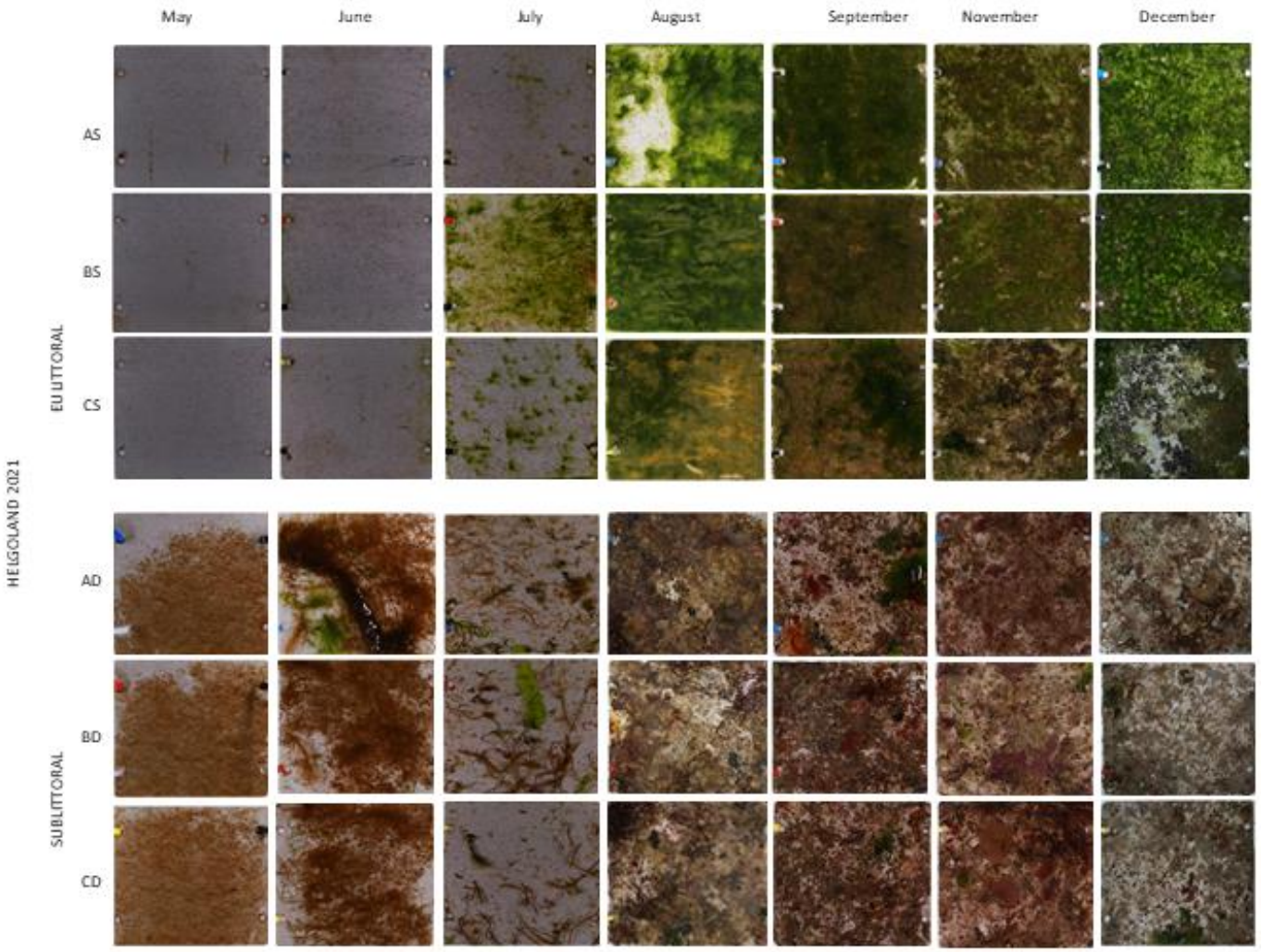

Figure 22 Monthly photographs of biofouling development for Helgoland in 2021 (HelEu and HelSub). Sampling was done from May until December (no sampling in October). Panel code: A, B, C; S - shallow (eulittoral), D - deep (sublittoral).

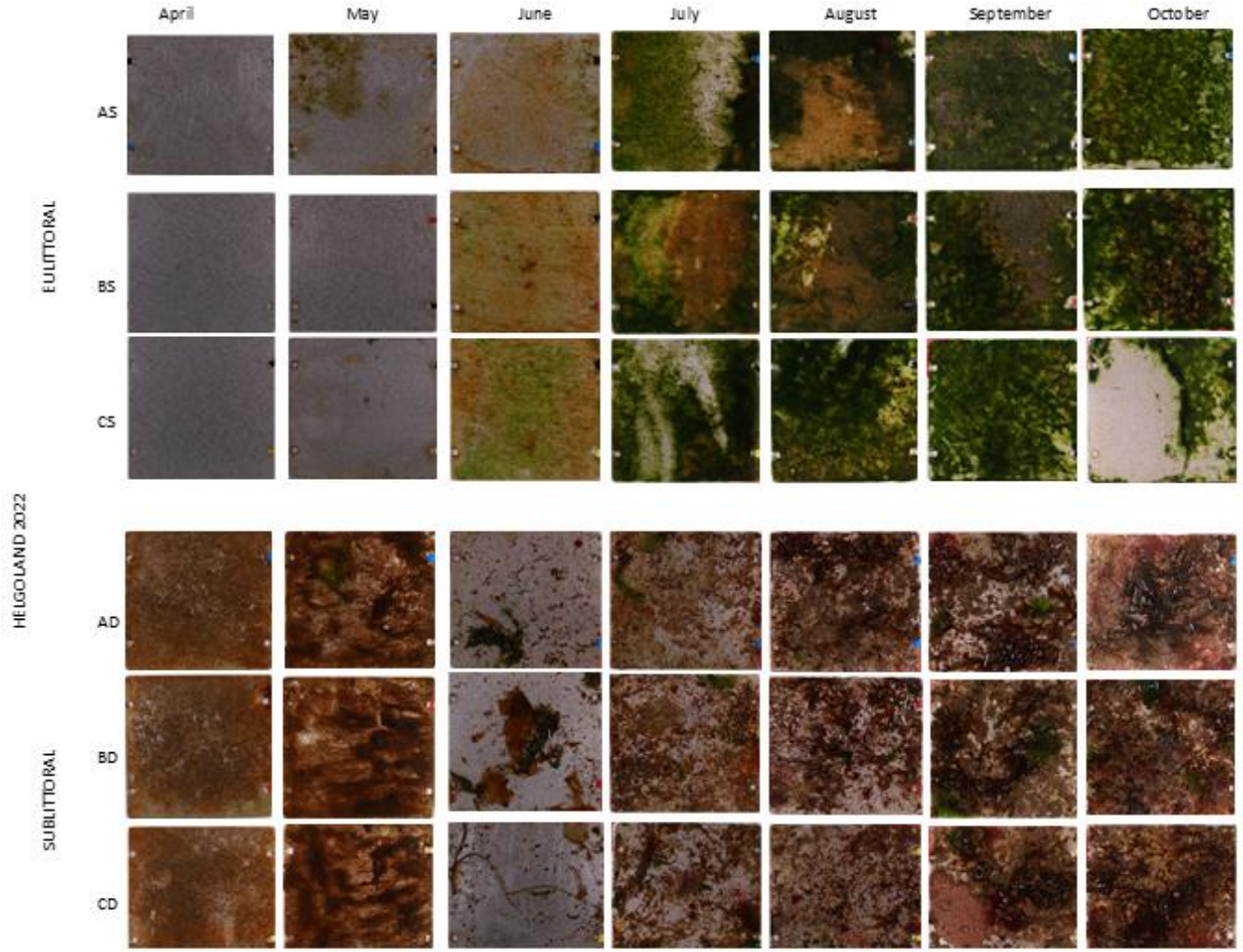

Figure 23 Monthly photographs of biofouling development for Helgoland in 2022 (HelEu and HelSub). Sampling was done from April until October. Panel code: A, B, C; S - shallow (eulittoral), D - deep (sublittoral).

7.3 Total coverage analysis using *ImageJ*

Table 9 Monthly total fouling coverage [%] for all panels of the Nordergründe site (A, B, C) for both years (excluding October in 2021) ± SD

Site NorSub21						Site NorSub22					
Sampling month	**Code Panel**	**Estimated fouling rate [%]**	***ImageJ* fouling rate [%]**	**Mean fouling rate per month *ImageJ* [%]**	**± SD *ImageJ* [%]**	**Sampling month**	**Code Panel**	**Estimated fouling rate [%]**	***ImageJ* fouling rate [%]**	**Mean fouling rate per month *ImageJ* [%]**	**± SD *ImageJ* [%]**
	A	45.00	23.53				A	85.00	95.85		
June	B	90.00	96.87	55.83	35.85	April	B	70.00	61.88	84.52	16.01
	C	55.00	47.09				C	90.00	95.83		
	A	95.00	94.68				A	100.00	100.00		
July	B	92.00	90.10	88.41	5.93	May	B	100.00	100.00	97.47	1.79
	C	74.00	80.45				C	95.00	96.20		
	A	100.00	100.00				A	100.00	100.00		
August	B	100.00	100.00	100	0	June	B	100.00	100.00	100	0
	C	100.00	100.00				C	100.00	100.00		
	A	98.00	96.99				A	100.00	100.00		
September	B	100.00	100.00	99	1.42	July	B	100.00	100.00	100	0
	C	100.00	100.00				C	100.00	100.00		
	A	100.00	100.00								
November	B	100.00	100.00	100	0						
	C	98.00	100.00								
total mean 2021				88.65	21.97	total mean 2022				95.5	10.38

Table 10 Monthly total fouling coverage [%] for all panels of the Helgoland site (A, B, C) in 2021 for both habitats (excluding October) ± SD

Site HelEu21						Site HelSub21					
Sampling month	Code Panel	Estimated fouling rate [%]	*ImageJ* fouling rate [%]	Mean fouling rate per month *ImageJ* [%]	± SD *ImageJ* [%]		Code Panel	Estimated fouling rate [%]	*ImageJ* fouling rate [%]	Mean fouling rate per month *ImageJ* [%]	± SD *ImageJ* [%]
	A	1.00	1.32				A	65.00	74.36		
May	B	0.50	0.92	0.81	0.47		B	80.00	90.23	86.75	9.04
	C	1.00	0.19				C	85.00	95.67		
	A	1.00	0.12				A	40.00	81.14		
June	B	1.00	0.17	1.11	1.37		B	50.00	75.42	78.77	2.43
	C	1.50	3.05				C	50.00	79.74		
	A	6.00	20.33				A	50.00	31.34		
July	B	75.00	60.91	32.28	20.33		B	33.00	54.15	35.43	13.92
	C	15.00	15.61				C	15.00	20.79		
	A	70.00	70.63				A	95.00	95.71		
August	B	100.00	100.00	90.21	13.85		B	95.00	86.99	92.49	3.91
	C	100.00	100.00				C	96.00	94.78		
	A	90.00	98.46				A	85.00	77.08		
September	B	98.00	98.78	98.87	0.38		B	85.00	90.30	83.64	5.4
	C	99.00	99.38				C	90.00	83.54		
	A	96.00	91.65				A	85.00	88.82		
November	B	100.00	96.09	92.96	2.22		B	90.00	86.09	87.76	1.19
	C	80.00	91.14				C	90.00	88.36		
	A	98.00	93.13				A	75.00	90.34		
December	B	95.00	92.95	86.37	9.43		B	75.00	83.41	83.72	5.28
	C	65.00	73.03				C	65.00	77.41		
total mean 2021				57.52	42.43					78.37	19.32

Table 11 Monthly total fouling coverage [%] for all panels of the Helgoland site (A, B, C) in 2022 for both habitats ± SD

Site HelEu22						Site HelSub22					
Sampling month	**Code Panel**	**Estimated fouling rate [%]**	***ImageJ* fouling rate [%]**	**Mean fouling rate per month *ImageJ* [%]**	**± SD *ImageJ* [%]**		**Code Panel**	**Estimated fouling rate [%]**	***ImageJ* fouling rate [%]**	**Mean fouling rate per month *ImageJ* [%]**	**± SD *ImageJ* [%]**
	A	1.00	0.66				A	70.00	94.84		
April	B	0.00	0.00	0.22	0.31		B	65.00	94.32	95.45	1.24
	C	0.00	0.00				C	60.00	97.18		
	A	20.00	21.24				A	90.00	88.2		
May	B	1.00	0.61	7.33	9.84		B	90.00	91.82	89.87	1.49
	C	2.00	0.13				C	95.00	89.59		
	A	47.00	98.58				A	35.50	22.91		
June	B	85.00	99.44	99.06	0.36		B	30.00	43.26	28.31	10.71
	C	90.00	99.16				C	19.00	18.75		
	A	83.00	79.45				A	85.00	73.58		
July	B	100.00	100.00	79.44	16.79		B	70.00	59.41	69.32	7.03
	C	75.00	58.87				C	85.00	74.96		
	A	99.00	99.14				A	86.00	91.08		
August	B	95.00	94.51	95.18	3.00		B	73.00	63.39	80.81	13.39
	C	98.00	91.89				C	75.00	87.97		
	A	97.00	96.49				A	80.00	78.33		
September	B	100.00	98.92	93.67	5.80		B	85.00	89.97	83.53	4.38
	C	95.00	85.59				C	90.00	82.29		
	A	91.00	93.33				A	97.00	97.51		
October	B	95.00	92.48	75.02	25.29		B	82.00	95.36	96.76	0.99
	C	35.00	39.26				C	98.00	97.4		
total mean 2022				63.98	41.03					77.72	23.07